An Application of the Chase Algorithm to Multiuser Detection

Liu, Feng

A Thesis

in

The Department

of

Electrical and Computer Engineering

Presented in Partial Fulfillment of the Requirements

for the Degree of Master of Applied Science at

Concordia University

Montreal, Quebec, Canada

April 2007

Your file Votre référence
ISBN: 978-0-494-34635-8
Our file Notre référence
ISBN: 978-0-494-34635-8

ABSTRACT

An Application of the Chase Algorithm to Multiuser Detection

Liu, Feng

With various added services in future wireless communication systems, the demand for fast and highly reliable data transmissions is continuously increasing. *Multiple access interference* (MAI) in *direct-sequence code division multiple acces*s (DS-CDMA) and constrained capacity in *single-input single-output* (SISO) are the major obstacles to achieve this purpose. For overcoming these limitations, the use of *multiuser detection* (MUD) and *multiple-input multiple-output* (MIMO) is necessary.

In the area of error control coding, the Chase algorithm, which takes advantage of the different reliabilities of the received symbols and focuses on correcting the error in the weakest symbols, can achieve a near *maximum-likelihood* (ML) performance and with significant complexity reduction. In this thesis, we discuss the application of the Chase algorithm in multiuser detectors for the SISO-CDMA and MIMO-CDMA systems.

In the SISO-CDMA systems, we develop a *parallel interference cancellation* (PIC) scheme using the Chase algorithm after the *matched filters* (MFs). This scheme is called Chase-PIC. Instead of optimizing the weight of each user as most of PIC detectors do, this detector provides a new optimizing approach right after the MFs. Based on the analysis of the complexity and performance over the flat and frequency-selective Rayleigh fading channels, we also propose a new Chase based multistage PIC that uses the *normalized least-mean-square* (NLMS) algorithm at the earlier stages and the Chase

algorithm at the later stages. This proposed scheme can achieve a better performance than NLMS-PIC but with less complexity.

In the MIMO-CDMA systems, we proposed a new Chase based multiuser detector over the flat Rayleigh fading channels. This detector focuses on correcting the error of the weakest detected symbol in the *layered space-time multiuser detector* (LAST-MUD). Compared to another Chase based detector, B-Chase, the proposed scheme has less complexity but with the tendency of achieving better performance at high *signal-to-noise ratio* (SNR).

ACKNOWLEDGEMENTS

First and foremost, I would like to express my greatest gratitude and thanks towards my supervisor, Professor Mohammad Reza Soleymani for all his patient guidance, kind encouragement and giving me a chance to work with him. His advice and suggestions on my research are very greatly appreciated. Without his valuable help, this project cannot be a success.

I also wish to extend my appreciation to my dear family. Because their support, I was able to focus on my study. A special acknowledgement is due to my mother. Without her great sacrifice and patience in taking care of my father, I could not be succeeding.

I would also like to give my thanks to my friends, Min Li, Yingzi Gao, Min Yang, Jijun He, Wei Wu for their valuable helps and encouragements.

Finally, thanks to my dear colleagues in the Wireless and Satellite Communication Lab. for helping me in many ways.

Dedicated to my dear parents...

Table of Contents

List of Tables

List of Figures

List of Abbreviations

Abbreviation	Definition
1G	first-generation
2G	second-generation
3G	third-generation
AMPS	advanced mobile phone service
AWGN	additive white Gaussian noise
BER	bit error rate
BLAST	Bell laboratories layered space-time
BPSK	binary phase-shift keying
CDMA	code division multiple access
DS-CDMA	direct-sequence code division multiple access
FDMA	frequency division multiple access
GSM	global system for mobile communication
IS	interim standard
ISI	intersymbol interference
ITU	international telecommunication union
LAST-MUD	layered space-time multiuser detector
LST	layered space-time
MAI	multiple access interference
MFs	matched filters
MIMO	multiple-input multiple-output
ML	maximum likelihood
MLSE	maximum-likelihood sequence estimation
MMSE	minimum mean-squared error
MSE	mean-squared error
MUD	multiuser detection
NLMS	normalized least-mean-square
NMT	nordic mobile telephony
PDC	personal digital cellular
PIC	parallel interference cancellation
PSD	power spectral density
QPSK	quadrature phase-shift keying
SIC	successive interference cancellation
SISO	single-input single-output
SNR	signal-to-noise ratio
ST	space-time
STBC	space-time block codes
STTC	space-time trellis codes
TACS	total access communications systems

TDMA	time division multiple access
TD-SCDMA	time division synchronous code division multiple access
V-BLAST	vertical Bell Laboratories layered space-time
WCDMA	wideband code division multiple access

CHAPTER 1

INTRODUCTION

After an exponential growth at the end of last century, the area of wireless communications is still one of the most promising and fast growing fields in the 21st century. The achievements of wireless communications are not only providing convenience for the people but also gradually changing people's lifestyles. In this chapter, first, we introduce the brief history of wireless communications [1]. Then we present two efficient techniques—*multiuser detection* (MUD) and *multiple-input multiple-output* (MIMO), which are used in the next generation wireless communication systems to enhance the system performance. Finally, we demonstrate the objectives and contributions of my thesis.

1.1 Brief History of Wireless Communications

The *first-generation* (1G) wireless communication systems were analog systems. They were deployed in the early 1980s and adopted the *frequency division multiple access*

(FDMA) technology. Various systems, such as *advanced mobile phone service* (AMPS), *total access communications system* (TACS) and *nordic mobile telephony* (NMT), belonged to this category. 1G systems were used only for voice communication and mainly suffered from two problems. The first one was the constrained capacity due to the reason that 1G systems serve only one subscriber at a time on a radio channel. Therefore, the number of available radio channels limited the system capacity. The second one was the limited bit rate since a very narrow radio channel, which varied from 10 kHz to 30 kHz, was provided in analog systems.

To cope with the problems of 1G systems, digital based *second-generation* (2G) wireless communication systems were developed. The use of digital signal significantly increased the spectrum efficiency compared to the analog systems. Two different multiple access techniques, *time division multiple access* (TDMA) and *code division multiple access* (CDMA), were adopted in different 2G systems. Compared to analog 1G systems that served only one subscriber on a radio channel, digital TDMA and CDMA systems can accommodate several subscribers on one radio channel, which increased the system capacity. The first developed 2G systems were based on TDMA. *Global System for Mobile Communication* (GSM), North American standard *Interim Standard* (IS) 54/136 and the Japanese standard *Personal Digital Cellular* (PDC) belong to this category. In these systems, the channel bandwidth ranges from 25 to 200 kHz. Based on CDMA, another leading 2G standard is cdmaOne (IS-95) whose channel bandwidth could be either a 30 kHz AMPS radio channel or a new 1.25 MHz CDMA channel.

The exponential growth of the Internet has resulted in requirement for new wireless multimedia services, which demand high-speed data packet transmissions. These new

services made the 2G systems, which were designed to provide good voice as well as basic data services, become inadequate. Hence, to cope with the need for higher capacity, the *third-generation* (3G) wireless communication systems were developed. All 3G systems are based on CDMA technology. Three standards were adopted by the *International Telecommunication Union* (ITU) for the 3G systems: *wideband code division multiple access* (WCDMA), *code division multiple access 2000* (CDMA2000) and *time division synchronous code division multiple access* (TD-SCDMA). These 3G systems can provide around 2 Mb/s indoors and 144 kb/s in vehicular environments, respectively.

In the future, with various added services, the demand for fast and high reliable data transmissions is continuously increasing. In current CDMA systems, this purpose can't be achieved due to *multiple access interference* (MAI) of CDMA and constrained capacity of conventional multiuser *single-input single-out* (SISO) systems. For overcoming these limitations, the effective interference cancellation technique, *multiuser detection* (MUD) and antenna array techniques, *multiple-input multiple-output* (MIMO), are the most powerful solutions.

1.2 Multiple Access Schemes

A multiple access scheme is the technique for sharing a limited network resource among different users as efficiently as possible. FDMA, TDMA and CDMA are three major multiple access techniques. In 1G and 2G systems, two types of multiple access techniques: FDMA and TDMA, were employed. In FDMA, the available spectrum was

divided into non-overlapping slots of frequency and each slot is assigned to one user. In TDMA, instead of aligning different users in different frequency slots, users are assigned to non-overlapping time slots. The main problem with both FDMA and TDMA is that they have hard capacity limits. It means when the number of users equals the number of frequency or time slots, adding one more user becomes impossible because all the available frequency or time resources have already been assigned to the existing users.

CDMA is a multiple access technique that can overcome this problem and lead to a large capacity increase. In this technique, users are multiplexed by distinct codes rather than by orthogonal frequency bands as in FDMA, or by orthogonal time slots as in TDMA. The most popular CDMA scheme is the *direct-sequence code division multiple access* (DS-CDMA) where each active user's data is directly modulated (multiplied) by a unique signature sequence (code). The systems that we will discuss in this thesis are also DS-CDMA systems.

1.3 Multiuser Detection

The performance of today's DS-CDMA systems is limited by *multiple access interference* (MAI) more than by any other single effect, such as noise. MAI happens when the signature waveforms assigned to different users are not orthogonal, which causes the performance degradation. *Multiuser detection* (MUD) is an enabling technique for mitigating MAI with the aim of improving system performance.

The functions of downlink and uplink receivers adopting the MUD technique are different [2]: in downlink, each mobile receiver only needs to detect its own signal.

Because all K user signals transmitted from the base station are synchronous and could be orthogonalized at the base station transmitter, there is no interference from intracell users, and the interference that needs to be suppressed comes from a few dominant neighbouring cells. In uplink, the situation becomes more complicated because the base station receiver must detect all desired users' symbols within one cell, and all the symbols transmitted from the mobile stations are asynchronous. Except the other-cell interference, the major interference that the base station receiver has to suppress comes from the intracell symbols. In this thesis, our research focuses on base station receivers used in the uplink situations.

The pioneering work of MUD has been done by Verdú [3]. He proposed an optimum detector based on the *maximum likelihood* (ML) detection principle. Hypothetically, this ML receiver would encompass a bank of matched filters that would produce a set of sufficient statistics, followed by a Viterbi decoder. Even though the ML receiver could achieve the substantial performance improvement compared to conventional matched filter receiver, its exponential complexity related to the user number is too high for practical DS-CDMA systems. Therefore, the goal of MUD research is to find the sub-optimum detectors that can achieve a good trade-off between performance and complexity.

The basic sub-optimum detectors are classified in two categories [4]: one is a linear detector and another is a subtractive interference cancellation detector. The linear multiuser detectors execute a linear transformation after the soft outputs of the conventional detector and achieve a complexity and performance trade-off between the conventional and optimum receivers. The decorrelating and the *minimum mean-squared*

error (MMSE) receivers are two typical linear multiuser detectors. The problem of the linear detector is the computation of matrix inversion that still requires high complexity. On the other hand, Subtractive interference cancellation detectors have a better structure in the sense of complexity. In this case, the interference of each user on the other users is estimated, re-spread, and cancelled from the received signal. These operations can be extended to multistages. The *successive interference cancellation* (SIC) and *parallel interference cancellation* (PIC) detectors are two well-known examples of this class. Normally, the SIC detector causes a longer delay and the PIC detector demands more hardware.

1.4 Multiple-Input Multiple-Output Systems

For the next generation of wireless systems, there are ever increasing demands for high data rates and improved reliability due to the integration of multimedia and Internet applications. Because of the limited available radio spectrum, the only way to achieve the higher data rates is to design more efficient signalling techniques. Compared to conventional single antenna link systems, the use of multiple antennas at both ends of the wireless link, well-known as MIMO systems, showed large gains in communication capacity [5, 6]. In general, for a MIMO system with an independent flat fading channel known at the receivers, the capacity grows linearly with the minimum number of antennas.

Like the Shannon capacity limit [7], references [5] and [6] only gave the information theoretical capacity limit of MIMO systems but no implementation scheme was

proposed. The space-time (ST) coding [8] is a set of effective and practical way to approaching this limit. The major issue of the space-time coding is to utilize the multipath effects to achieve high spectral efficiency and performance gains. So far, different space-time coding structures have been proposed [9], which include space-time block codes (STBC), space-time trellis codes (STTC), space-time turbo trellis codes and layered space-time (LST) codes.

1.5 The Motivation and Objective

In the optimum ML multiuser detector of CDMA systems, we assume that all users' symbols have the same reliability and choose the final decision from 2^K possible hard decision vectors, where K is the number of active users in the systems. The application of the optimum multiuser detector for CDMA systems is undesirable due to the exponential high complexity. This high complexity could be avoided by using the Chase algorithm [10] that was originally used in a channel block decoder with channel information. The success of the Chase algorithm is based on a reality that the detected symbols have different reliabilities at the receiver side. Therefore, we can keep the detected symbols with high reliabilities intact but try different hard decision combinations for the least reliable user data, and then select the final hard decision values based on a smaller set.

The objective of this thesis is to develop the Chase based MUD schemes in the SISO and MIMO-CDMA uplink systems.

1.6 Contributions of This Thesis

The main contributions of this thesis are the following:

- We derive a PIC scheme using the Chase algorithm after the *matched filters* (MFs). This scheme is called Chase-PIC.
- We assess the complexity and performance analysis. Based on this analysis, we propose a new Chase based multistage PIC scheme over synchronous Rayleigh fading channels. This new scheme benefits from the advantages of the Chase-PIC and the adaptive multistage *normalized least-mean-square parallel interference cancellation* (NLMS-PIC) [11]. This proposed scheme can achieve a good trade-off between performance and complexity.
- We extend the proposed Chase based multistage PIC scheme to asynchronous Rayleigh fading channels.
- We analyze the performance of MIMO-CDMA systems over synchronous Rayleigh fading channels using B-Chase and L-Chase [12] that were originally developed in single-user *vertical Bell Laboratories layered space-time* (V-BLAST) systems [13].
- We analyze the selection criterion of the weakest symbol in MIMO-CDMA systems and propose a new Chased based multiuser detector that has a tendency to achieve a better performance than the B-Chase detector at a high *signal-to-noise ratio* (SNR) while with less complexity.

1.7 Thesis Organization

This thesis is continued as follows.

Chapter 2 reviews three techniques: CDMA MUD, MIMO and the Chase algorithm. In the section of the MUD technique, we first introduce a conventional detector using a single-user detection strategy. And then, the optimum ML detector is presented. After that, two categories of sub-optimum MUD detectors are demonstrated, which include linear and subtractive detectors. The following section explains the basic principles of the Chase algorithm used in a block decoder. In the final section, we introduce some single-user MIMO techniques that include V-BLAST and the Chase detectors.

Chapter 3 presents the new multistage PIC schemes using the Chase algorithm. Our discussion will be divided into synchronous and asynchronous Rayleigh fading channels. In the synchronous situation, first of all, we derive a Chase-PIC detector. And then, different PIC schemes combining the Chase and NLMS algorithms are presented and their performances and complexities are compared with NLMS-PIC scheme. Finally, a scheme with pure NLMS used in the earlier stage and pure Chase algorithm used in the later stage is proposed. This proposed scheme can achieve better performance than multistage NLMS-PIC but with less complexity. In the asynchronous channels, the demonstration of our proposed scheme is straightforward.

Chapter 4 shows a novel Chase-based multiuser detector over MIMO-CDMA systems. In this chapter, we first discuss the use of B-Chase and L-Chase in MIMO-CDMA systems, which were two Chase based detectors originally used in single-user V-BLAST systems. Moreover, we point out the problem in the B-Chase and L-Chase

detectors. Finally, we carry out the mathematical analysis for the choice criterion of the most unreliable symbol and propose a new Chase-based multiuser detector. This new scheme has less complexity than the B-Chase detector but with the tendency of achieving better performance at a high SNR.

Chapter 5 concludes this thesis and some suggestions for future works are included.

CHAPTER 2

BACKGROUND

In this chapter, we review three techniques used in this thesis, which include *multiuser detection* (MUD), the Chase algorithm and *multiple-input multiple-output* (MIMO). In Section 2.1, various multiuser detectors for the direct-sequence code division multiple access (DS-CDMA) systems are presented. Section 2.2 presents the Chase algorithm used in the block decoder. In Section 2.3, we start with the introduction of MIMO techniques and one typical MIMO scheme—*vertical Bell Laboratories layered space-time* (V-BLAST). And then, the Chase detectors in single-user MIMO channel are demonstrated.

2.1 CDMA Multiuser Detectors

This section reviews the basic multiuser detection techniques in DS-CDMA systems. The outline of this section is as follows: In Subsection 2.1.1, the synchronous DS-CDMA multiuser system model is presented. Subsection 2.1.2 describes the

conventional detector and the idea of MUD. Subsection 2.1.3-7 investigate five multiuser detection schemes: the optimum *maximum-likelihood* (ML), the decorrelating, the *minimum mean-squared error* (MMSE), the *successive interference cancellation* (SIC) and *parallel interference cancellation* (PIC) detectors. Subsection 2.1.8, 9 introduce two improved PIC detectors—the partial PIC and adaptive *normalized least-mean-square* PIC (NLMS-PIC) detectors.

2.1.1 System Model

In this section, for the sake of simplicity, the following assumptions will be made concerning a DS-CDMA system:

- The channel attenuation is represented by a real value. This assumption simplifies the analysis and can be easily extended to the complex case. In Chapter 3, we will use fading channels where complex attenuation needs to be considered.
- Perfect channel estimation is assumed. This means that the parameters related to the channels are known at a receiver and the receiver can take advantage of the known parameters.
- At the receiver, the spreading codes used to do a correlation are perfectly synchronous with the received signals.

We consider a synchronous DS-CDMA system model shown in Fig. 2.1. There are K users communicating with the same rate over a channel corrupted by *additive white Gaussian noise* (AWGN). The baseband received signal can be written as

$$r(t)=\sum_{i=1}^{K} s_i(t)+z(t) = \sum_{i=1}^{K} A_i a_i c_i(t) + z(t). \tag{2.1}$$

If we consider sampling the continuous received signal at the chip rate N, (2.1) can be rewritten as:

$$r(m) = \sum_{i=1}^{K} A_i a_i c_i(m) + z(m). \tag{2.2}$$

Here, A_i is the signal amplitude. a_i is the ith user's data bit; *binary phase-shift keying* (BPSK) modulation is assumed and $a_i \in \{1,-1\}$. $c_i(t)$ is the signature waveform (spreading code) and its amplitude $c_i(m) \in \{1/\sqrt{N}, -1/\sqrt{N}\}$, where N is the processing gain (or spreading factor); $c_i(t)$ is assumed to have a unit energy, i.e. $\int_0^{T_b} \|c_i(t)\|^2 dt = 1$ or $\sum_{m=0}^{N-1} \|c_i(m)\|^2 = 1$, where T_b is the signal interval of a user bit. $z(t)$ is AWGN with zero-mean and two-sided power spectral density (PSD) of $N_o/2$ watts per hertz.

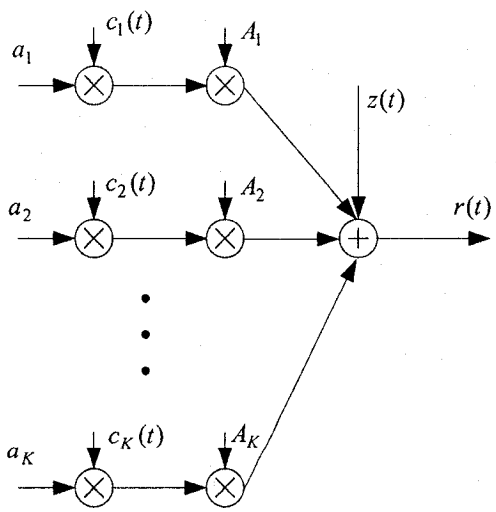

Figure 2.1 A synchronous DS-CDMA system model

It is also convenient to represent (2.2) in vector form

$$\mathbf{r} = \mathbf{CAa} + \mathbf{z}, \tag{2.3}$$

where $\mathbf{r}$ is a column vector of length N; $\mathbf{C}$ is a $N \times K$ matrix and $\mathbf{C} = [\mathbf{c}_1, \mathbf{c}_2, \cdots, \mathbf{c}_K]$, here $\mathbf{c}_i$ is the length N column vector associated with the ith user, $i \in \{1, 2, \cdots, K\}$; $\mathbf{A} = diag[A_1, A_2, \cdots, A_K]$; $\mathbf{a} = [a_1, a_2, \cdots, a_K]^T$ is the data vector and "T" denotes matrix transpose; $\mathbf{z}$ is the channel noise vector with covariance $\sigma_n^2\mathbf{I}$ and $\mathbf{I}$ is $N \times N$ identity matrix.

2.1.2 Conventional Single-User Detector

In this subsection, we first review the conventional single-user detector. The technique used in the conventional detector is a single-user detection strategy. The term of "single-user" here doesn't mean that there is only one user in a system; it means each branch detects one user without regarding the existence of other users. While introducing the conventional single-user detector, we also show the problem of *multiple access interference* (MAI) existing in this detector. After that, the idea of MUD, which has the purpose of migrating MAI, is described.

As shown in Fig 2.2, the conventional single-user detector consists of a bank of K correlators. The implementation of each correlator is the same as a matched filter [14]. In each detector branch, the signature waveform of one user is regenerated and correlated with the received signal. The output of the ith correlator, which is denoted as $\tilde{a}_i$,

$i \in \{1, 2, \cdots, K\}$, is the soft decision of the ith user's data. According to the sign of the soft decision, the hard decision $\hat{a}_i$ is made.

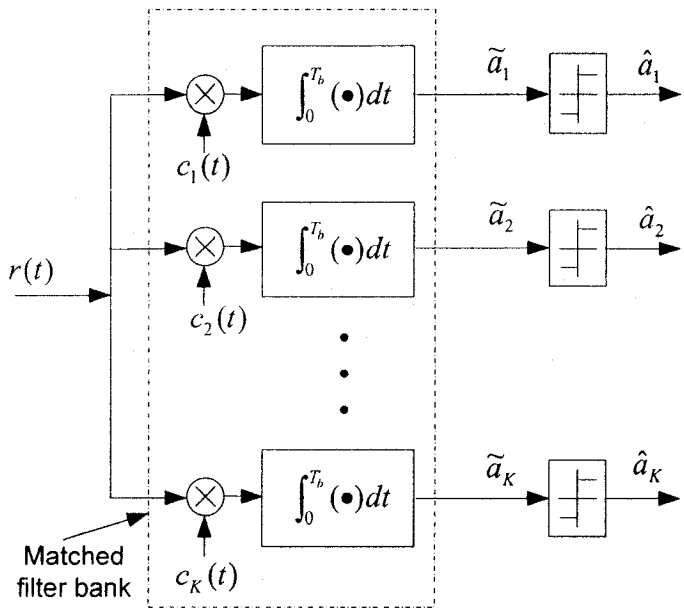

Figure 2.2 The conventional detector of a DS-CDMA system

After the conventional matched filter bank, the output can be written as

$$\tilde{a}_i = \int_0^{Tb} r(t)c_i(t)dt$$

$$= \int_0^{Tb} [\sum_{j=1}^{K} A_j a_j c_j(t) + z(t)]c_i(t)dt$$

$$= A_i a_i + \sum_{\substack{j=1 \\ j\neq i}}^{K} A_j a_j \rho_{j,i} + n_i \,, \tag{2.4}$$

where $\rho_{j,i}$ is a correlation coefficient and n_i is a noise term after despreading. $\rho_{j,i}$ and n_i are expressed as

$$\rho_{j,i} = \int_0^{T_b} c_j(t)c_i(t)dt = \sum_{m=0}^{N-1} c_j(m)c_i(m), \tag{2.5}$$

and

$$n_i = \int_0^{T_b} z(t)c_i(t)dt = \sum_{m=0}^{N-1} z(m)c_i(m). \tag{2.6}$$

The right-hand side of (2.4) consists of three parts: the desired signal $A_i a_i$, MAI $\sum_{\substack{j=1 \\ j\neq i}}^{K} A_j a_j \rho_{j,i}$ and the noise n_i. The conventional detector treats MAI as another noise and the estimated data $\hat{a}_i$ for a_i is

$$\hat{a}_i = \text{sgn}\{\tilde{a}_i\}. \tag{2.7}$$

The matrix-vector notation of the matched filter bank output is

$$\tilde{\mathbf{a}} = \mathbf{C}^T\mathbf{r} = \mathbf{C}^T(\mathbf{CAa} + \mathbf{z}) = \mathbf{RAa} + \mathbf{n}, \tag{2.8}$$

here, $\tilde{\mathbf{a}} = [\tilde{a}_1, \tilde{a}_2, \cdots, \tilde{a}_K]^T$, $\mathbf{n} = [n_1, n_2, \cdots, n_K]^T$ are the length K vector that hold the matched filter output and noise. The matrix $\mathbf{R}$ is a $K \times K$ matrix, whose entries contain the values of the correlations between each pair of codes.

We can break the matrix $\mathbf{R}$ into two $K \times K$ matrices: $\mathbf{R} = \mathbf{I} + \mathbf{Q}$. Here, $\mathbf{I}$ is a identity matrix and presents the autocorrelations of the spreading codes; $\mathbf{Q}$ contains the off-diagonal elements of $\mathbf{R}$ and denotes the crosscorrelations of the spreading codes. Parallel to (2.4), we can rewrite (2.8) as

$$\tilde{\mathbf{a}} = \mathbf{RAa} + \mathbf{n} = (\mathbf{I} + \mathbf{Q})\mathbf{Aa} + \mathbf{n} = \mathbf{Aa} + \mathbf{QAa} + \mathbf{n}, \tag{2.9}$$

where the first term $\mathbf{Aa}$ is the recovered data weighted by the received amplitudes; the second term $\mathbf{QAa}$ shows MAI, the interference from other users.

MAI has a major impact on the capacity and performance of the conventional DS-CDMA system. If the users' signals reach the receiver with different powers, the effect of MAI on system performance is more significant. The strong users' signals could bury a weaker user's signal. This is known as the near-far problem. In a fading channel, the near-far problem also arises.

For mitigating the effect of MAI, some techniques are suggested in [4], which include: designing the code waveform with as low cross-correlation as possible, using power control, designing powerful forward error correction codes, using sectored/adaptive antennas, using MUD. Our thesis will discuss MUD. The meaning of MUD is to share multiuser information and do joint signal processing. The general block diagram of a multiuser detector is shown in Fig. 2.3.

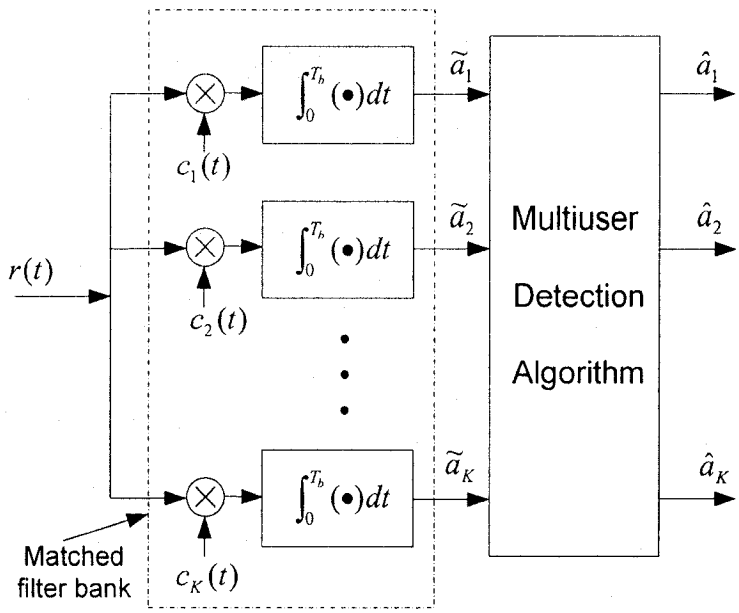

Figure 2.3 The block diagram of a multiuser detector

2.1.3 Optimum Multiuser Detector

The optimum multiuser detector uses the *maximum-likelihood sequence estimation* (MLSE) approach. Using the simplified DS-CDMA system model in Subsection 2.1.1, the *maximum-likelihood* (ML) solution is the decision vector $\hat{\mathbf{a}} = [\hat{a}_1, \hat{a}_2, \cdots, \hat{a}_K]^T$ maximizing [3]

$$\exp(-\frac{1}{2\sigma^2}\int_0^{T_b}[r(t)-\sum_{i=1}^{K}A_i c(t)\hat{a}_i]^2\,dt). \tag{2.10}$$

In another word, it is to minimize

$$\int_0^{T_b}[r(t)-\sum_{i=1}^{K}A_i c(t)\hat{a}_i]^2\,dt. \tag{2.11}$$

Assuming perfect synchronization, the equation (2.11) can be rewritten in a discrete form as

$$\sum_{m=0}^{N-1}\left|r(m)-\sum_{i=1}^{K}A_i c_i(m)a_i\right|^2. \tag{2.12}$$

In synchronous DS-CDMA system, the optimum detector finds the solution $\hat{\mathbf{a}}$ by exhaustive search, i.e. calculating the Euclidean distance between the received signal and the 2^K possible bit patterns, and choosing the one that minimizes (2.12). The optimum detector provides the most reliable decision and its performance is superior to all other detectors. But unfortunately, this kind of detector has exponential complexity with the number of users. When there are a large number of users, this approach becomes too complex to implement. Therefore, various sub-optimum multiuser detectors that have reasonable performance degradation but with less complexity have been proposed. Two major categories of sub-optimum detectors are linear detector and subtractive interference

cancellation detector. The deccorelating detector and the *minimum mean-squared error* (MMSE) detector are two typical linear detectors. The *successive interference cancellation* (SIC) detector and the *parallel interference cancellation* (PIC) detector belong to the class of subtractive interference cancellation detector. All these sub-optimum detectors are introduced in the following subsections.

2.1.4 Decorrelating Detector

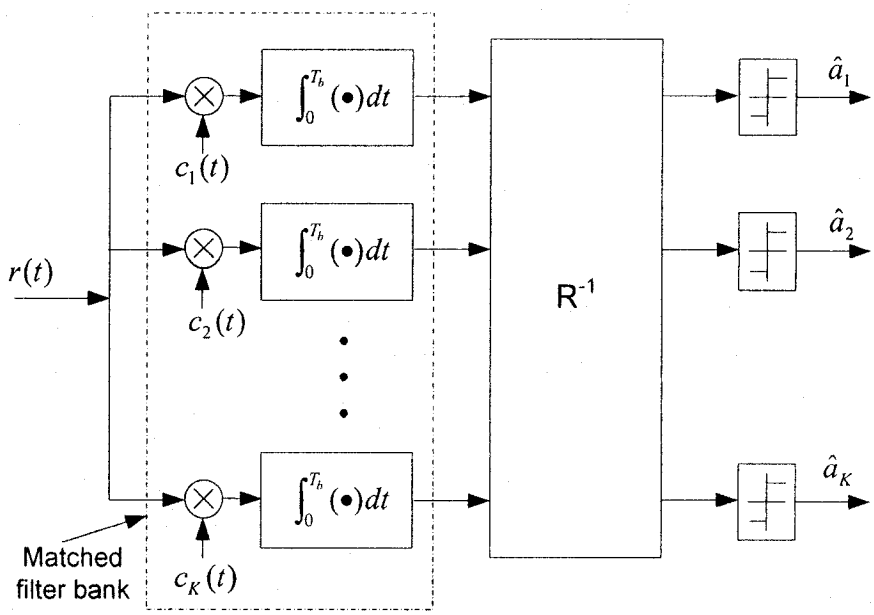

Figure 2.4 The decorrelating detector

The decorrelating detector is a linear detector and its block diagram is shown in Fig. 2.4. In this detector, $\mathbf{R}^{-1}$, the inverse of the correlation matrix $\mathbf{R}$, is applied to the output of the conventional detector. Hence, the transmitted data is decoupled. From (2.8), the soft output of this detector is

$$\tilde{\mathbf{a}}_{dec} = \mathbf{R}^{-1}(\mathbf{RAa} + \mathbf{n}) = \mathbf{Aa} + \mathbf{R}^{-1}\mathbf{n} = \mathbf{Aa} + \mathbf{n}_{dec}, \tag{2.13}$$

where $\tilde{\mathbf{a}}_{dec}$ is a length K column vector. Equation (2.13) shows that MAI is completely eliminated in the decorrelating detector. This detector is very similar to the zero-forcing equalizer [14] that is used to completely eliminate *intersymbol interference* (ISI).

The decorrelating detector was initially proposed in [15, 16]. The further analysis of this detector was done by Lupas and Verdú in [17, 18]. The advantages and disadvantages properties of the decorrelating detector are listed below [4]:

Advantages:

- Offers substantial performance/capacity gains over the conventional detector.
- Doesn't require the knowledge of the received amplitudes and is resistant to the near-far problem.
- Has much less computational complexity than that of the optimum ML detector.

Disadvantages:

- Causes noise enhancement that is similar to the zero-forcing equalizer [14].
- Has a high computational complexity in inverting the matrix $\mathbf{R}$, especially for asynchronous systems.

2.1.5 Minimum Mean-Squared Error (MMSE) Detector

The MMSE detector [19] is another kind of linear detector whose structure is shown in Fig. 2.5. The difference between the decorrelating detector and the MMSE detector is that the MMSE detector takes into account the background noise and the knowledge of the received signal powers but the decorrelating detector doesn't. A linear mapping $\mathbf{L}_{MMSE}$ is applied after MFs, which can minimize $E[|\mathbf{a} - \mathbf{L}_{MMSE}\tilde{\mathbf{a}}|^2]$, the mean-squared

error between the actual data and the soft output of the MFs. The expression for $\mathbf{L}_{MMSE}$ is

$$\mathbf{L}_{MMSE}=[\mathbf{R}+(N_0/2)\mathbf{A}^{-2}]^{-1}. \tag{2.14}$$

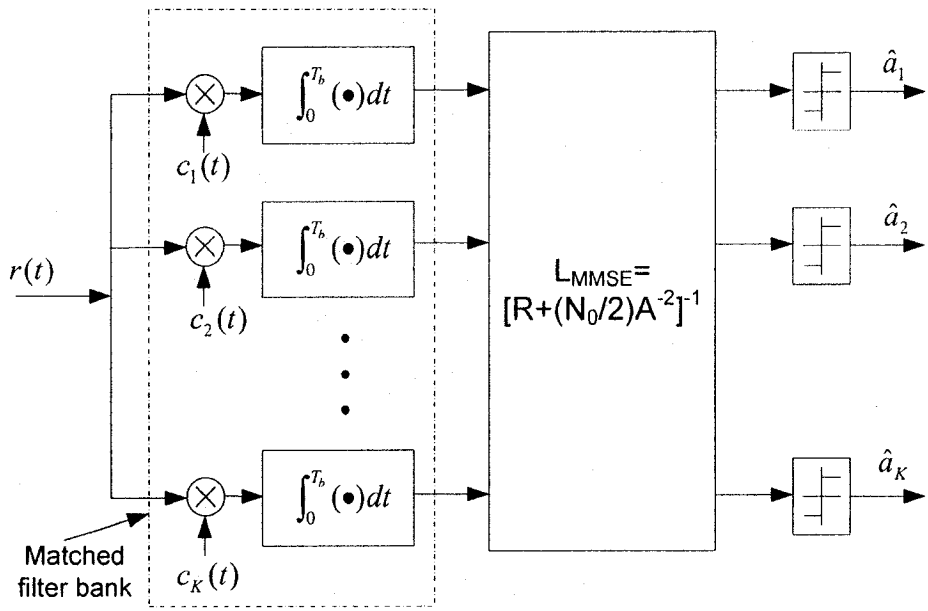

Figure 2.5 The MMSE detector

The MMSE detector is similar to the MMSE linear equalizer used to combat ISI [14]. The desire for eliminating MAI completely and the desire of not enhancing the background noise are balanced in the MMSE detector.

The advantages and disadvantages of the MMSE detector are demonstrated below:

Advantage:

- The MMSE detector has a better performance than the decorrelating detector because it takes the background noise into account.

Disadvantages:

- Requires the estimation of the received amplitudes.
- Is less resistant to the near-far problem.
- Needs implementation of matrix inversion.

2.1.6 Successive Interference Cancellation (SIC) Detector

The SIC detector [20, 21] is one class of subtractive interference cancellation detectors. The successive nature of this kind of detector is based on the following idea: In the conventional detector using single-user detection strategy, the user with strongest power at the receiver side has less possibility of making wrong decision and its presence causes major MAI when detecting other users' data. If we can estimate the strongest user's data correctly and cancel it completely from the received signal, other users, especially the weakest user, will have huge reductions in their MAI.

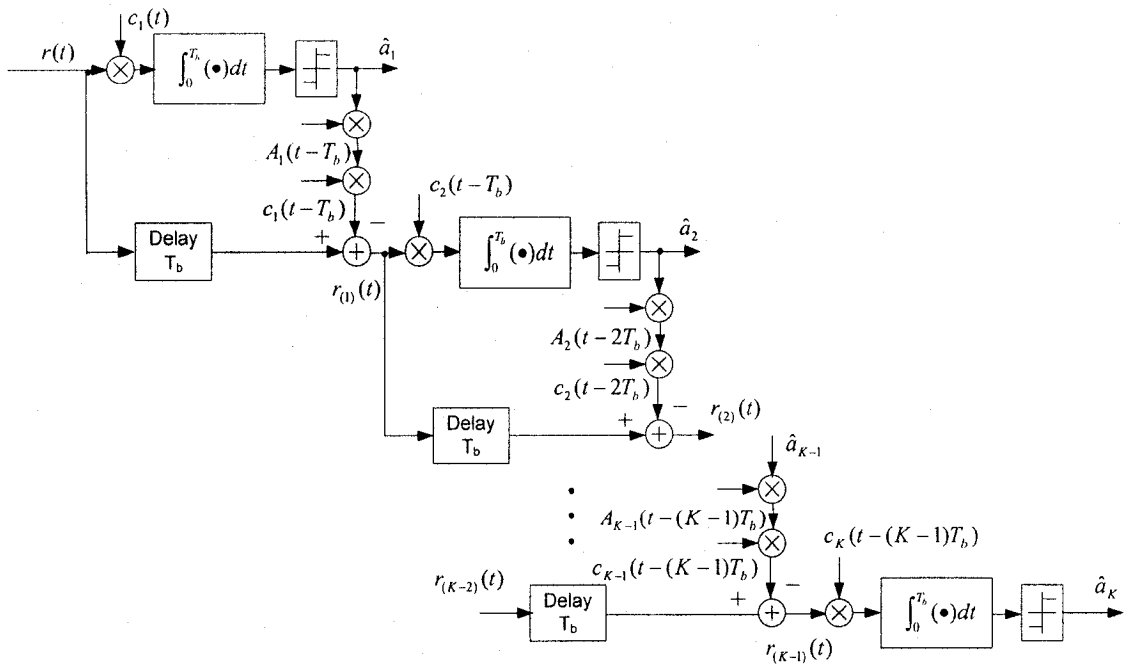

Figure 2.6 The successive interference cancellation (SIC) detector

In the SIC detector, first, an operation that ranks the user signals powers in descending order is executed. After that, K serial stages are utilized to estimate user data. Each stage decides one user data and cancels it from the remaining received signal. The user data detection order is the same as the descending order of the received powers, i.e. the strongest user data is detected first, and then the second strongest user data is detected, and so on. In each stage, this detector detects, regenerates, and cancels out one user's data from the received signal; hence, the remaining users have less MAI in the next stage. Depending on the soft decision or hard decision of each user's data is used to estimate the interference, the SIC detectors are divided into the soft and hard SIC detector. Fig. 2.6 shows the simplified diagram of the hard SIC detector. Before the first stage, there is an operation (not shown in the diagram) that ranks the signals in descending order of their received powers. Some small time delays are also ignored in Fig. 2.6.

Advantages:

- It offers a low complexity scheme compared to all other types of multiuser detectors.
- There is a high chance to get the correct data decision for the strongest user because achieving acquisition and demodulation on the strongest user is easier.
- The elimination of the strongest users gives huge MAI reduction and most benefit for the remaining users.

Disadvantages:

- One bit duration delay happens when detecting each user.

- Reordering the signals is necessary whenever the power profile changes
- An erroneous decision on the strongest user will be propagated through all other users' decision.
- Its performance degrades apparently when there is no significant power variation among each users' received signal.

2.1.7 Total Parallel Interference Cancellation (PIC) Detector

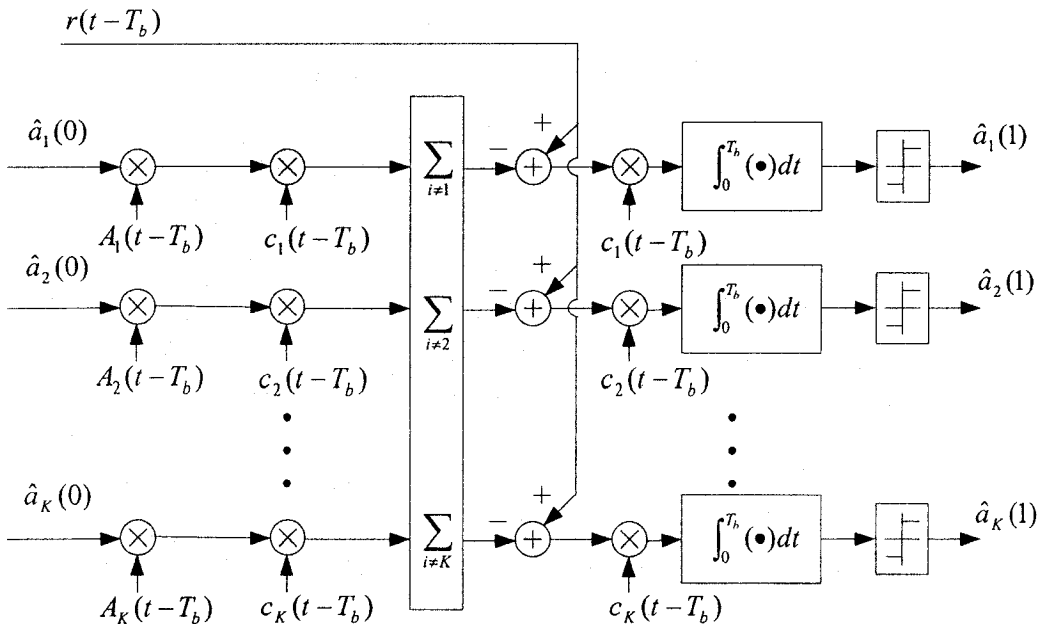

Figure 2.7 The total parallel interference cancellation (PIC) detector (one stage)

In contrast to the SIC detector, the PIC detector [22] adopts a parallel approach and eliminates all MAI affecting the users. In other words, all users' data are estimated and re-spread at the same time and the MAI originating from other users are cancelled from the received signal at once. The PIC process can be extended to multistage where all

stages have the same structure. Similar to the SIC detector, there are also soft PIC and hard PIC. Fig. 2.7 shows one stage of a hard PIC detector. This scheme can also be defined as total PIC because it utilizes a total interference cancellation approach. In this approach, the interference to each user, which is from all other users, is estimated and completely cancelled in each stage.

Advantages:

- It is faster than the SIC detector.
- It is much simpler than the optimum and linear detectors.

Disadvantages:

- It is more complex than the SIC detector.
- It is more vulnerable to near-far problem than the SIC detector since the users' data with different power are detected at the same time.

Multistage PIC is a good candidate for real-world implementation due to the fact that it has less processing delay than SIC and involves a simpler structure compared to the linear detectors. In this thesis, multistage PIC scheme is chosen as further study.

2.1.8 Partial Parallel Interference Cancellation Detector

In the total PIC approach introduced in Subsection 2.1.7, the interference to each user, which is from all other users, is estimated and completely cancelled in each stage. In fact, this approach is not the best philosophy since wrongly estimated interference may be cancelled in the earlier stage and the performance improvement could not be guaranteed.

A better approach is to assign a weight to each user. In this subsection, partial PIC [23], a scheme adopting the weight assigning philosophy, is introduced.

In each stage, instead of cancelling the entire amount of estimated multiuser interference in total PIC, partial PIC only cancels a fraction of multiuser interference by introducing a weight factor p_k. In the earlier stages, the interference estimate is poor, a small value of p_k is used. In the later stages, the value of p_k increases since more reliable estimated user data is available. In the sense of multistage implementation, the kth stage of the partial PIC detector is shown in Fig. 2.8.

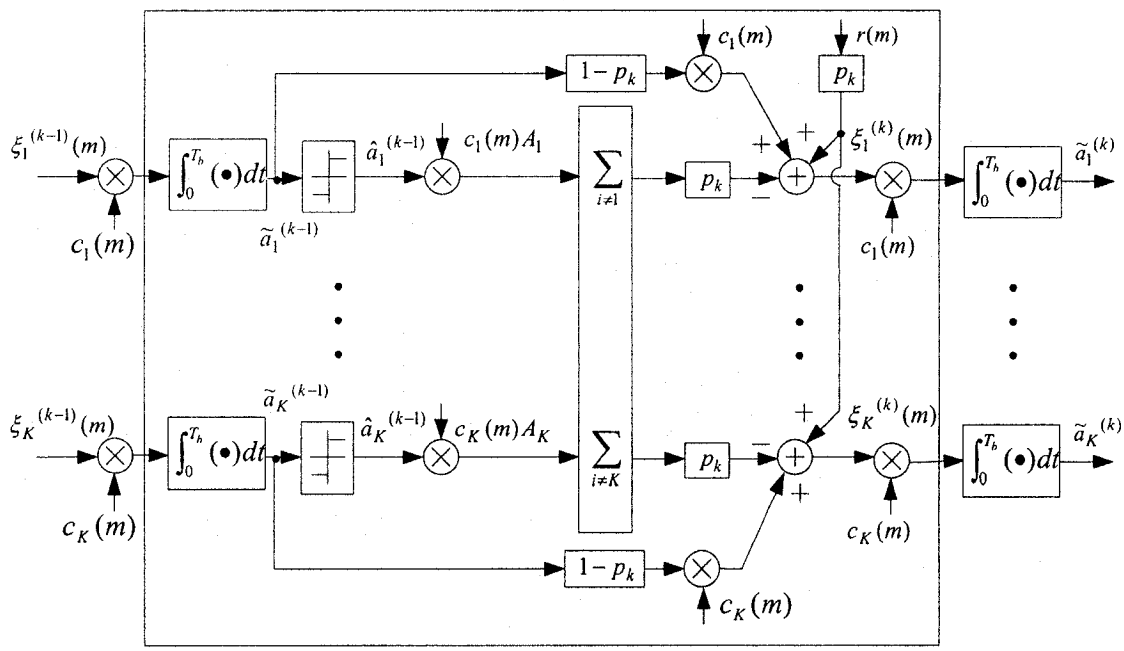

Figure 2.8 The *k*th stage of the partial parallel interference cancellation detector

Here, $\xi_i^{(k-1)}(m)$ is the chip information of user i after interference cancellation in stage $k-1$. When $k-1=0$, $\xi_i^{(k-1)}(m)=r(m)$.

A soft decision of the ith user of the kth stage is

$$\tilde{a}_i^{(k)} = p_k[\tilde{a}_i^{(0)} - \sum_{\substack{j=1 \\ j\neq i}}^{K}\left(\int_0^{T_b} \hat{a}_j^{(k-1)} c_j(t) c_i(t) A_i\, dt\right)] + (1-p_k)\tilde{a}_i^{(k-1)}$$

$$= p_k[\tilde{a}_i^{(0)} - \sum_{\substack{j=1 \\ j\neq i}}^{K}\left(\hat{a}_j^{(k-1)} A_i \rho_{j,i}\right)] + (1-p_k)\tilde{a}_i^{(k-1)} \qquad (2.15)$$

2.1.9 Adaptive Normalized Least-Mean-Square Parallel Interference Cancellation (NLMS-PIC) Detector

The shortcoming of partial PIC is that the weights are identical for all users in each stage and they may not appropriately indicate the reliability of the estimated user bits. For reflecting the reliability of data estimation, it is more reasonable to have different weights from one user to another and from bit to bit. Therefore, Xue et al. proposed an adaptive PIC scheme [11] using normalized least-mean-square (NLMS) algorithm to update the weight of each user within one stage. The kth stage of NLMS-PIC is shown in Fig. 2.9 and its weight updating for the weighting vector $\boldsymbol{\lambda}^{(k)} = (\lambda_1^{(k)}, \lambda_2^{(k)}, \cdots, \lambda_K^{(k)})^T$ is illustrated in Fig. 2.10.

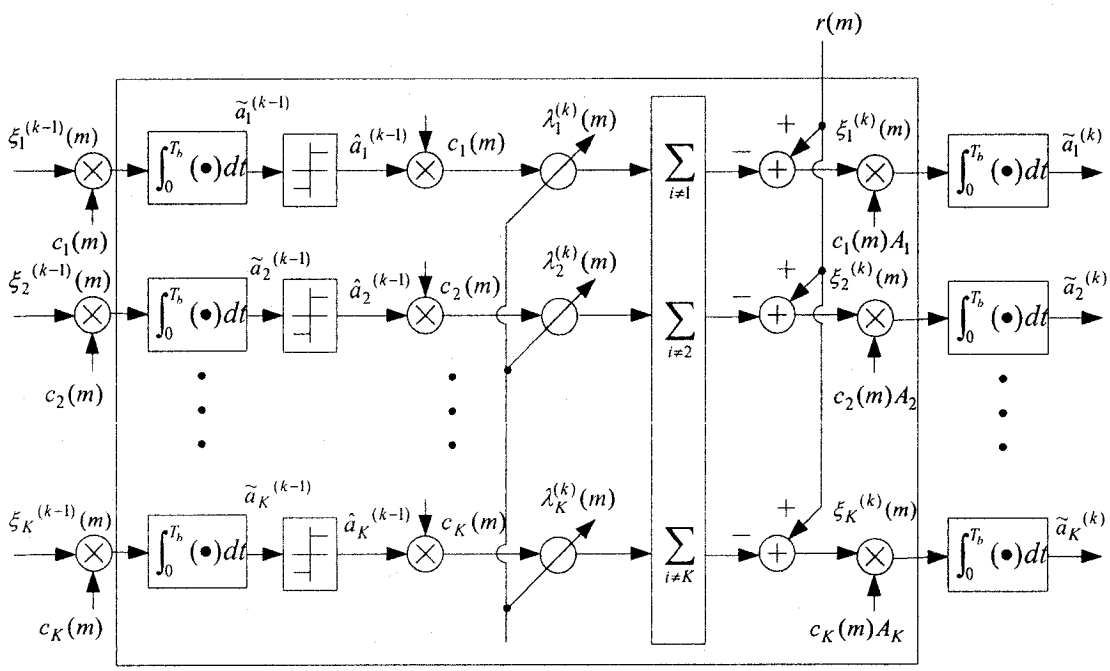

Figure 2.9 The *k*th stage of the NLMS-PIC detector

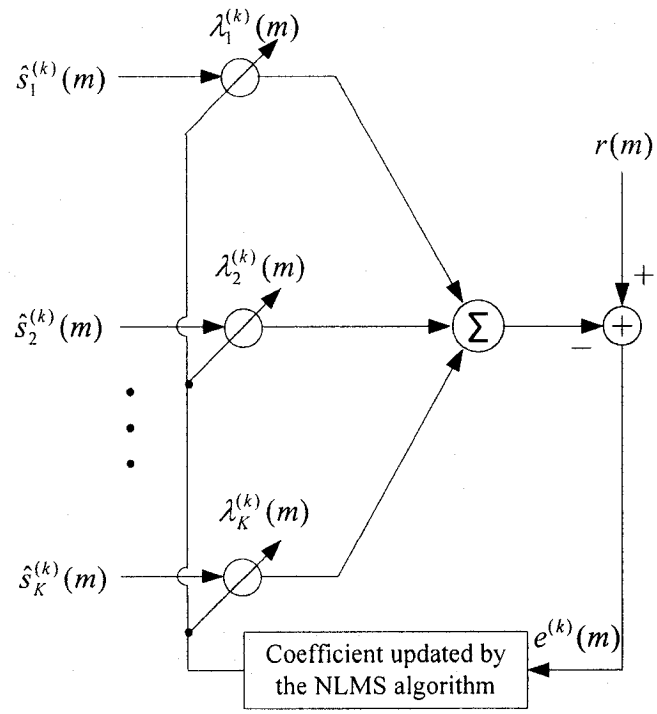

Figure 2.10 Weight updating in the adaptive NLMS-PIC detector

The NLMS algorithm is based on the *mean-squared error* (MSE) criteria. In the kth stage, the NLMS-PIC detector looks for a weight vector $\boldsymbol{\lambda}^{(k)} = (\lambda_1^{(k)}, \lambda_2^{(k)}, \cdots, \lambda_K^{(k)})^T$ which can minimize the MSE between the received signal $r(m)$ and the estimated signal $\hat{r}(m)$. In another word, the weight vector should satisfy a cost function as follows:

$$\min_{\boldsymbol{\lambda}^{(k)}} E\left[\left|r(m) - \hat{r}^{(k)}(m)\right|^2\right]$$

$$= \min_{\boldsymbol{\lambda}^{(k)}} E\left[\left|r(m) - \sum_{i=1}^{K} c_i(m)\hat{a}_i^{(k-1)}\lambda_i^{(k)}(m)\right|^2\right], \tag{2.16}$$

here, $\hat{r}^{(k)}(m)$ is the estimate of the received signal in the kth stage, $\hat{a}_i^{(k-1)}$ is the estimate of a_i in the $(k-1)$th stage. The updating operation of the weight vector $\boldsymbol{\lambda}^{(k)}$ is performed in a bit interval and on a chip basis as follows:

$$\boldsymbol{\lambda}^{(k)}(m+1) = \boldsymbol{\lambda}^{(k)}(m) + \frac{\mu}{\left\|\hat{\mathbf{s}}^{(k)}(m)\right\|^2}\left[\hat{\mathbf{s}}^{(k)}(m)\right]e^{(k)}(m), \tag{2.17}$$

where the initial values of $\boldsymbol{\lambda}^{(k)}$ could be the estimated channel coefficients, μ is a step size, column vector $\hat{\mathbf{s}}^{(k)}$ is the input of the NLMS algorithm in the kth stage, and its ith entry is written as

$$\hat{s}_i^{(k)}(m) = c_i(m)\hat{a}_i^{(k-1)}. \tag{2.18}$$

In (2.17), $e^{(k)}(m)$ denotes the error of the received signals and its estimate in the kth stage and is written as

$$e^{(k)}(m) = r(m) - \hat{r}^{(k)}(m). \tag{2.19}$$

For each bit, weight vector is updated until $m = N-1$. Therefore, the interference cancellation is carried out by using $\boldsymbol{\lambda}^{(k)}(N-1)$. After the interference cancellation, the residual signals corresponding to the ith user in the ith stage is written as

$$\xi_i^{(k)}(m) = r(m) - \sum_{\substack{j=1 \\ j \neq i}}^{K} \lambda_j^{(k)}(N-1)\hat{s}_j^k(m). \tag{2.20}$$

$\xi_i^{(k)}(m)$ can be sent to the next stage or directly sent to conventional MFs and make a decision for the transmitted user data.

2.2 Chase Algorithm

The Chase algorithm [10] was originally proposed for decoding block codes with channel measurement information. In block decoder, conventional binary decoding has small error correcting capability. The optimum decoder is the one adopting the ML approach but unfortunately the high complexity prevents its application. The decoder using the Chase algorithm achieves a good trade-off between binary decoder and the ML decoder, which has the ability to correct more error number than conventional binary decoding and requires less complexity than the ML decoder.

In this section, the basic idea of the Chase algorithm is introduced by using the case of block decoder. At the beginning, the system model, the binary decoding and ML decoding are introduced. And then, Chase algorithm is demonstrated.

2.2.1 System Model of a Codec Communication System

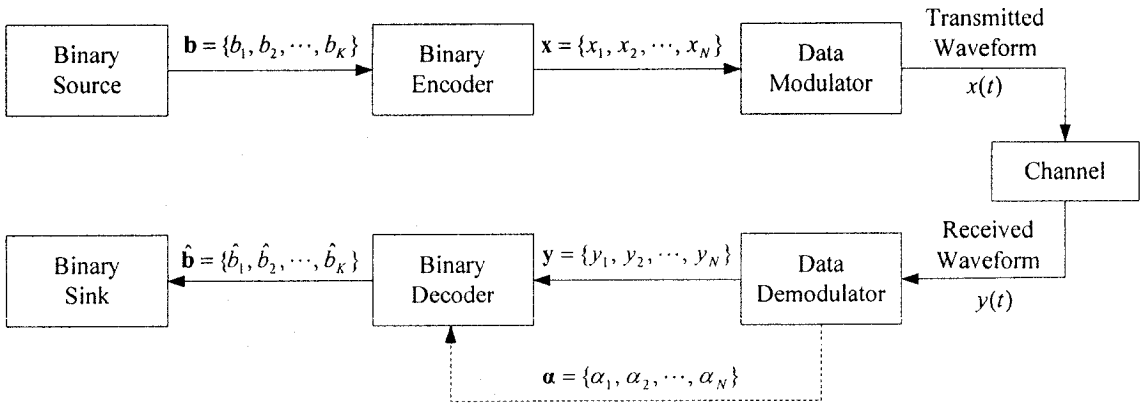

Figure 2.11 A Codec communication system block diagram

The model of a codec communication system is shown in Fig. 2.11. For simplicity, assume the transmission of block coded binary symbols {-1, +1} using BPSK modulation over an AWGN channel. A binary sequence $\mathbf{b} = \{b_1, b_2, \cdots, b_K\}$, which has K binary information digits, is encoded into a block of N binary digits denoted by $\mathbf{x} = \{x_1, x_2, \cdots, x_N\}$. After the data modulator and channel, two outcomes are produced by the data demodulator: one is $\mathbf{y} = \{y_1, y_2, \cdots, y_N\}$, a sequence of N binary digits; another is the channel measurement information $\boldsymbol{\alpha} = \{\alpha_1, \alpha_2, \cdots, \alpha_N\}$, a sequence of N positive number. The entry of $\boldsymbol{\alpha}$ denotes a measure of the reliability of corresponding received binary digits in $\mathbf{y}$. In another word, if $\alpha_i > \alpha_j$, y_i is more likely to be correct than y_j.

The conventional binary decoder doesn't use the channel measurement information and has the ability correcting up to $\lfloor (d-1)/2 \rfloor$ errors, where d is the minimum

Hamming distance of the code and $\lfloor (d-1)/2 \rfloor$ denotes the greatest integer less than or equal to $(d-1)/2$. Assume $\mathbf{z}_m = \{z_{m1}, z_{m2}, \cdots, z_{mN}\}$ is the error sequence to indicate the difference between the received sequence $\mathbf{y}$ and a codeword $\mathbf{x}_m = \{x_{m1}, x_{m2}, \cdots, x_{mN}\}$, which contains a 1 in the places where $\mathbf{y}$ and $\mathbf{x}_m$ differ.

$$\mathbf{z}_m = \mathbf{y} \oplus \mathbf{x}_m = \{y_1 \oplus x_{m1}, y_2 \oplus x_{m2}, \cdots, y_N \oplus x_{mN}\}, \tag{2.21}$$

where the notation "$\oplus$" is the modulo-2 addition. If we define the binary weight of a sequence $\mathbf{z}_m$ as

$$W(\mathbf{z}_m) = \sum_{i=1}^{N} z_{mi}, \tag{2.22}$$

the function of the conventional binary decoder is to find the codeword satisfy

$$W(\mathbf{z}_m) = W(\mathbf{y} \oplus \mathbf{x}_m) \le \lfloor (d-1)/2 \rfloor. \tag{2.23}$$

If (2.23) is satisfied, the codeword will be unique; otherwise, no codeword will be found. In the conventional binary decoder, the detailed description for finding the codeword is in [14] and is not shown in this thesis.

Taking account the channel measurement information $\boldsymbol{\alpha} = \{\alpha_1, \alpha_2, \cdots, \alpha_N\}$, we can define the analog weight of the error sequence $\mathbf{z}_m$ as

$$W_\alpha(\mathbf{z}_m) = W_\alpha(\mathbf{y} \oplus \mathbf{x}_m) = \sum_{i=1}^{N} \alpha_i z_{mi} = \sum_{i=1}^{N} \alpha_i (y_i \oplus x_{mi}). \tag{2.24}$$

The ML decoder checks all codewords and choose the one minimizing (2.24) as the final codeword, i.e. finds the codeword that can satisfy

$$\min_m W_\alpha(\mathbf{z}_m), \tag{2.25}$$

where the range of m is over all codewords.

The decision given by the ML decoder is optimum, but the complexity increasing exponentially with the block size K makes this approach prohibitive when K is a big number.

2.2.2 Chase Algorithm in Block Decoder

As a decoder using channel measurement information, the Chase algorithm proposed a sub-optimum solution, which can achieve near ML performance but with significant complex reduction. In contrast to the conventional binary decoder, which consider only one error pattern, the Chase based decoder uses a binary decoder to help obtain a small set of possible error patterns and chooses the error pattern having minimum analog weight defined by (2.25). The detailed description of the Chase algorithm in block decoder is as follows:

Step 1: Create a set of test patterns.

Taking the error correct capacity up to $\lfloor d-1 \rfloor$ as an example, three test pattern selection algorithms were proposed [10] in the Chase algorithm. In the sequence of algorithm 1, 2, and 3, the complexity becomes less but the performance becomes inferior. Among these three approaches, algorithm 2 is a good candidate for application, which has performance close to algorithm 1 but with less complexity. Thus, in the rest of this thesis, the Chase algorithm will be used is based on algorithm 2. The test pattern $\mathbf{t}$ is produced by filling any combination of 1 to the $\lfloor d/2 \rfloor$ positions, which has lowest channel measurement values, i.e. lowest confident values.

Step 2: Produce a set of candidate codeword

By adding (modulo-2) the test pattern created in last step to the received sequence $\mathbf{y}$, a new sequence $\mathbf{y}'$ is obtained and

$$\mathbf{y}' = \mathbf{y} \oplus \mathbf{t}. \tag{2.26}$$

Using the conventional binary decoding, a new error pattern $\mathbf{z}'$, which corresponds to $\mathbf{y}'$, is created. Therefore, based on the received sequence $\mathbf{y}$, a set of actual error pattern is given by

$$\mathbf{z}_t = \mathbf{t} \oplus \mathbf{z}'. \tag{2.27}$$

In another word, we can say that a set of candidate codeword is produced because one error pattern $\mathbf{z}'$ relative to one codeword.

Step 3: Determine the codeword

Substitute (2.27) into (2.25), choose the code word that can achieve minimum value as the final codeword. This determined codeword matches the received sequence best among the candidate codeword set.

Although ML decoder considers all the channel measurement information, it doesn't take advantage of the property of this information, which relates to the reliability of received bits. The ML decoder has high complexity due to the reason that it considers all the received bits have identical reliabilities. The Chase based decoder makes use of different reliability information of the received bits. The received bits with high confidence values are kept intact and the least reliable bits are replaced by all possible combinations. The function using in the ML decoder to determine the final codeword is also applied in Chase decoder while the determination is made on a smaller set.

2.3 Multiple-Input Multiple-Output (MIMO) Communication Systems

In the next generation of wireless systems, there is an ever increasing demand for high data rate and improved reliability due to the integration of multimedia and Internet applications. Because the limited available radio spectrum, the only way to achieve the higher data rates is to design more efficient signalling techniques. Compare to conventional single antenna link systems, recent research in information theory shown that MIMO systems have potential to achieve large capacity gain [5, 6]. The MIMO channel uses multiple antennas at both ends of a wireless link, and its capacity could grow linearly with the minimum number of antennas.

So far, various MIMO architectures, such as *space-time block codes* (STBC) [24, 25, 26], *space-time trellis codes* (STTC) [27], *Bell Labs. layered space-time* (BLAST) systems [28, 29] and smart antenna beamforming [30], have been proposed. In this thesis, our research is related to one of the BLAST systems, known as *vertical Bell Laboratories Layered Space-Time* (V-BLAST). In Subsection 2.3.1, the V-BLAST system model and its detection algorithm are presented. In Subsection 2.3.2, we introduces two Chase based detectors that ameliorate V-BLAST system performance when the number of transmit antennas is equal to the number of receive antennas.

2.3.1 V-BLAST System

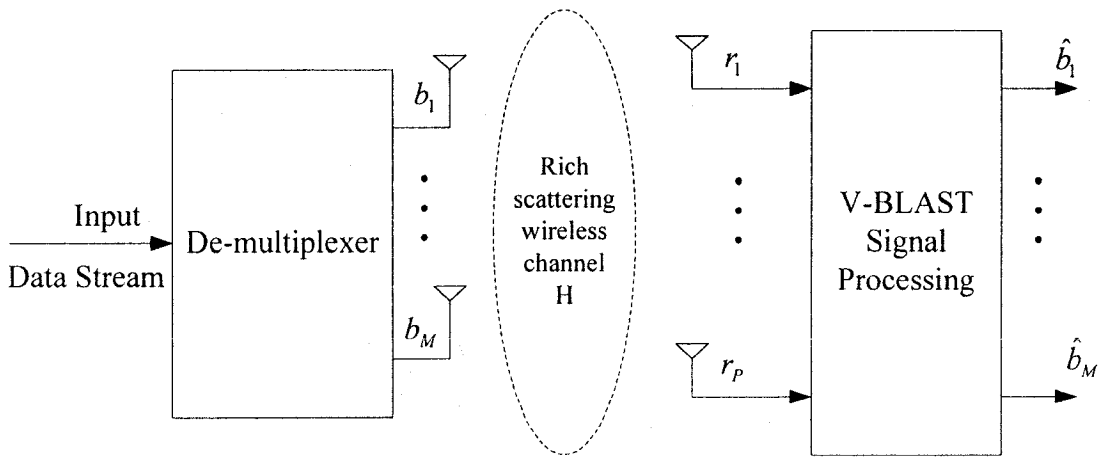

Figure 2.12 V-BLAST system block diagram

A block diagram of the V-BLAST system is shown in Fig. 2.12. This system is a single user system. The number of transmit antennas is M and the number of receive antennas is P. At the transmitter side, a single user input data stream first pass through a de-multiplexer; after that, M substream symbols are sent through M antennas. The transmitted symbols can be represented as a length M vector $\mathbf{b} = [b_1, \ldots, b_M]^T$ where each entry is the symbol transmitted from a single antenna. The channel matrix $\mathbf{H} = [\mathbf{h}_1, \mathbf{h}_2, \cdots, \mathbf{h}_M]$ is a $P \times M$ complex matrix, where the ith column $\mathbf{h}_i$ is a length P vector; each entry $h_{i,j}$ is the complex coefficient between transmit antenna j and receive antenna i. Therefore, the baseband received signal can be written as

$$\mathbf{r} = \mathbf{Hb} + \mathbf{n}, \tag{2.28}$$

where $\mathbf{r} = [r_1, r_2, \cdots, r_P]^T$ is a complex vector of length P. The noise is represented by $\mathbf{n}$, a length P complex zero-mean AWGN noise vector with the covariance matrix $\sigma^2 \mathbf{I}_P$, where $\mathbf{I}_P$ denotes the $P \times P$ identity matrix.

The V-BLAST algorithm [29] utilizes iteration approach, and the iteration number is equal to the number of the transmit antenna of the system. At each iteration, the user symbol with maximum post-detection *signal-to-noise ratio* (SNR) is detected and eliminated from the received signals. References [13, 29] pointed out that the smallest post-detection SNR in all iteration dominates the error performance of the system. Therefore, the optimum detection order is the one that maximize the minimum post-detection SNR, which is so-called the global optimization. The global optimization method need to evaluate $M!$ stacking options to decide the decision order, while the proposed V-BLAST detection scheme find the decision order by considering $\sim M^2/2$ options. References [13, 29] also proved that the proposed V-BLAST scheme equals global optimization

The detailed description of the V-BLAST detection algorithm [29] is as follows:

$$\text{for } i = 1 \text{ to } M \tag{2.29a}$$

$$k_i = \arg \min_{j \notin \{k_1, \cdots, k_{i-1}\}} \left\| [\mathbf{H}(i)^+]_j \right\|^2 \tag{2.29b}$$

$$\mathbf{w}_{k_i} = [\mathbf{H}(i)^+]_{k_i} \tag{2.29c}$$

$$z_{k_i} = \mathbf{w}_{k_i} \mathbf{r}(i) \tag{2.29d}$$

$$\hat{b}_{k_i} = \psi(z_{k_i}) \tag{2.29e}$$

$$\text{if } i \le M - 1 \tag{2.29f}$$

$$\mathbf{r}(i+1) = \mathbf{r}(i) - [\mathbf{H}(i)]_{k_i} \hat{b}_{k_i} \tag{2.29g}$$

end (2.29*h*)

obtain $\mathbf{H}(i+1)$ (2.29*i*)

$i \leftarrow i+1$ (2.29*j*)

end . (2.29*k*)

Here, i denotes the ith iteration and + denotes the Moore-Penrose pseudoinverse. The notation $[\mathbf{H}(i)^+]_j$ represents the jth row of matrix $\mathbf{H}(i)^+$. The nulling vector $\mathbf{w}_{k_i}$ is a length-P row vector and generated by taking out $[\mathbf{H}(i)^+]_{k_i}$. $\mathbf{H}(i+1)$ is obtained by zeroing column k_i of $\mathbf{H}(i)$.

At each iteration, the V-BLAST algorithm consists of four steps that are described below:

Step 1: Determination of the optimal ordering, (2.29*b*).

The user that corresponds to the minimum norm of the row vector of $\mathbf{H}(i)^+$ is chosen as the detected user in current iteration. This user has maximum post-detection SNR and the lowest possibility to make a wrong decision compared to other existing users. The proof of this statement is as follows:

Assume the row of $\mathbf{H}(i)^+$, which corresponds to the undetected data in the system, has the index k_i. A nulling vector is constructed by taking out corresponding row of $\mathbf{H}(i)^+$, i.e. $\mathbf{w}_{k_i} = [\mathbf{H}(i)^+]_{k_i}$. If there is no wrong decision in the previous detected data and the effect of these data is cancelled completely from the received signals. The soft decision of the k_ith symbol is

$$z_{k_i} = \mathbf{w}_{k_i}\mathbf{r}(i) = \mathbf{w}_{k_i}[\mathbf{H}(i)\mathbf{b}(i) + \mathbf{n}] = \mathbf{w}_{k_i}\mathbf{H}(i)\mathbf{b}(i) + \mathbf{w}_{k_i}\mathbf{n} = b_{k_i} + \mathbf{w}_{k_i}\mathbf{n}, \quad (2.30)$$

here, $\mathbf{b}(i)$ is obtained by taking out the user data detected in previous from original transmitted data vector $\mathbf{b}$.

The desired symbol power is $\|b_{k_i}\|^2$, the noise power is

$$E[\|\mathbf{w}_{k_i}\mathbf{n} - E(\mathbf{w}_{k_i}\mathbf{n})\|^2, \quad (2.31)$$

here,

$$E(\mathbf{w}_{k_i}\mathbf{n}) = E(\mathbf{w}_{k_i})E(\mathbf{n}) = E(\mathbf{w}_{k_i})\mathbf{0} = 0. \quad (2.32)$$

Substitute (2.32) into (2.31),

$$\begin{aligned} & E[\|\mathbf{w}_{k_i}\mathbf{n} - E(\mathbf{w}_{k_i}\mathbf{n})\|^2 \\ & = E[\|\mathbf{w}_{k_i}\mathbf{n} - 0\|^2 = E[\|\mathbf{w}_{k_i}\mathbf{n}\|^2] = E[(\mathbf{w}_{k_i}\mathbf{n})(\mathbf{w}_{k_i}\mathbf{n})^H] \\ & = E[\mathbf{w}_{k_i}\mathbf{n}\mathbf{n}^H\mathbf{w}_{k_i}^H] = \mathbf{w}_{k_i}E[\mathbf{n}\mathbf{n}^H]\mathbf{w}_{k_i}^H = \mathbf{w}_{k_i}\sigma^2\mathbf{I}_{P\times P}\mathbf{w}_{k_i}^H \\ & = \sigma^2\|\mathbf{w}_{k_i}\|^2. \end{aligned} \quad (2.33)$$

Therefore, the post-detection SNR is

$$\rho_{k_i} = \frac{\|b_{k_i}\|^2}{\sigma^2\|\mathbf{w}_{k_i}\|^2}, \quad (2.34)$$

here, σ^2 is a constant. If *quadrature phase-shift keying* (QPSK) modulation is assumed, $\|b_{k_i}\|^2$ is a constant. Therefore, the smaller of $\|\mathbf{w}_{k_i}\|^2$, the larger of ρ_{k_i}. If $k_i = \arg\min_{j\in\{k_1,\cdots,k_{i-1}\}}\|[\mathbf{H}(i)^+]_j\|^2$, ρ_{k_i} has the maximum value, i.e. maximum post-detection SNR.

Step 2: Nulling vector computation, (2.29*c*).

Step 3: Signal estimation, (2.29*d*), (2.29*e*).

Equations (2.29*d*), (2.29*e*) are the hard decision, soft decision of the desired user data respectively.

Step 4: Interference cancellation, (2.29*f*)~(2.29*j*).

2.3.3 Chase Based Detectors

The performance of the V-BLAST algorithm can approach the performance of the ML detector when the number of receive antennas is more than the number of transmit antennas. Otherwise, the V-BLAST detector is significantly inferior to the ML detector [12]. The research that aims at reducing the gap in performance between V-BLAST and ML detector has been proposed in [31, 32, 12]. In this subsection, we will review the B-Chase and L-Chase detectors, which belong to a family of Chase detectors [12]. Both the B-Chase and L-Chase detectors can outperform the V-BLAST detector and the L-Chase detector requires less complexity.

2.3.3.1 B-Chase detector

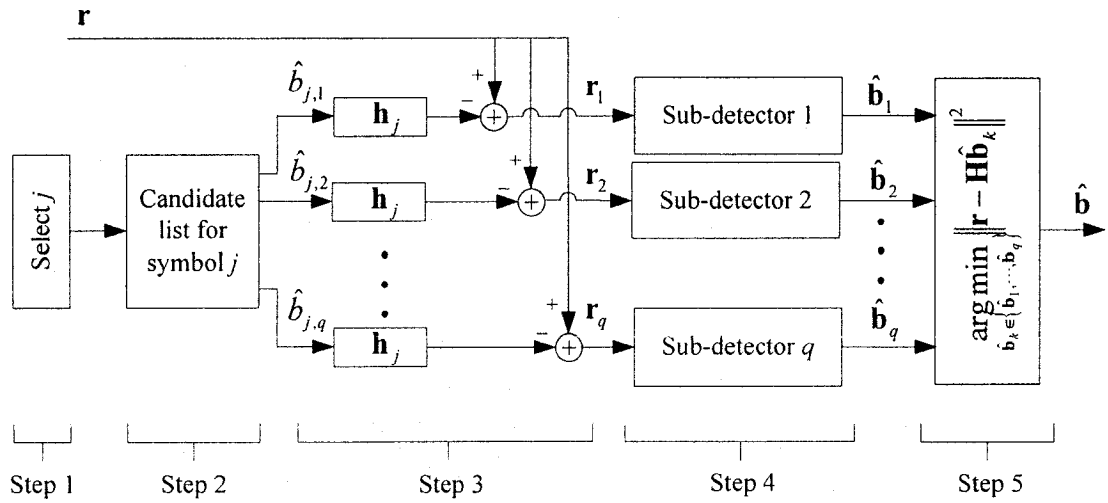

Figure 2.13 The block diagram of the B-Chase detector

From [12], the block diagram of the B-Chase detector is shown in Fig. 2.13 and its detection procedure is defined by five steps:

Step 1: Identify the first detected symbol

The index of the first detected symbol is assumed to be j and $j \in \{1,\cdots,M\}$. If we want that the subdetectors perform well as much as possible when making decisions about the remaining $M-1$ symbols, the choice of j should make $\mathbf{h}_j$, one column of $\mathbf{H}$, least orthogonal to the other column of $\mathbf{H}$. In this case, the index j corresponds to the row of $\mathbf{H}^+$ with maximum norm $\|\mathbf{w}_j\|$. In another word, the first detected symbol in the B-Chase detector is the one with minimum post-detection SNR at the first iteration of the V-BLAST algorithm.

Step 2: Generate a candidate value list $\{\hat{b}_{j,1}, \hat{b}_{j,2}, \cdots, \hat{b}_{j,q}\}$ for the first detected symbol.

The value q is an integer with the range from 1 to the size of signal modulation constellation. With a signal modulation constellation, the large value of q, the better detection performance is obtained.

Step 3: Determine a set of q residual vectors $\{\mathbf{r}_1, \mathbf{r}_2, \cdots, \mathbf{r}_q\}$.

The residual vectors are produced by cancelling the contribution of the first detected symbol from $\mathbf{r}$, where the residual vector is calculated by

$$\mathbf{r}_i = \mathbf{r} - \mathbf{h}_j b_{j,k}. \tag{2.35}$$

Step 4: Send each residual vector to its corresponding sub-detector and make the decision for the left $M-1$ symbols.

The sub-detector of B-Chase is the same as the V-BLAST detector, which is the reason that we have the name of B-Chase. By combining with the first detected symbol $\hat{b}_{j,k}$, the output of the kth sub-detector is a candidate hard decision vector $\hat{\mathbf{b}}_k$.

Step 5: Choose the final decision $\hat{\mathbf{b}}$ that can satisfy a cost function

$$\arg\min_{\hat{\mathbf{b}}_k \in \{\hat{\mathbf{b}}_1, \cdots, \hat{\mathbf{b}}_q\}} \left\| \mathbf{r} - \mathbf{H}\hat{\mathbf{b}}_k \right\|^2. \tag{2.36}$$

The detection procedure of the B-Chase detector is similar to the Chase algorithm for soft decoding. The Chase algorithm in decoder begins by identifying the $\lfloor d/2 \rfloor$ least reliable bits of a received codeword and creating the test patterns. This is analogous to Step 1, except in Step 1, only one symbol is identified instead of $\lfloor d/2 \rfloor$ and there is no test pattern. And then, the Chase algorithm creates $2^{\lfloor d/2 \rfloor}$ candidate codewords, which is

similar to Step 2. Finally, the Chase algorithm chooses a codeword among the candidate set, which is analogue to the Steps 3, 4 and 5.

2.3.3.2 L-Chase Detector

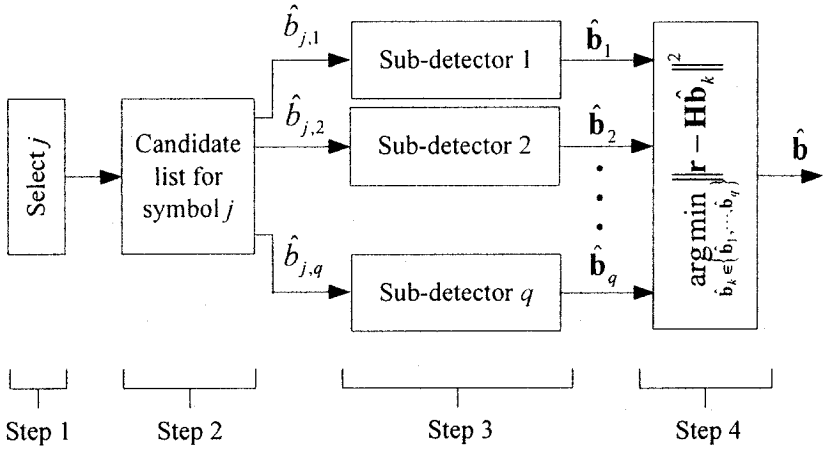

Figure 2.14 The block diagram of the L-Chase detector

The block diagram of the L-Chase detector [12] is shown in Fig. 2.14. The L-Chase detector only has two differences from the B-Chase detector. The first one is that there is no Step 3 of B-Chase in L-Chase, i.e. the candidate values $\{\hat{b}_{j,1}, \cdots, \hat{b}_{j,q}\}$ are sent to sub-detectors directly. The second one is the sub-detector's operation of L-Chase focuses on estimating and cancelling the noise terms, which is quite different from the operation of the B-Chase sub-detector. The reason with the name of L-Chase is that the sub-detector here is so-called linear detector. The detailed description of the operation of the L-Chase sub-detector is shown below.

Let

$$\mathbf{c} = \mathbf{H}^{+}\mathbf{r} = \mathbf{H}^{+}(\mathbf{H}\mathbf{b} + \mathbf{n}) = \mathbf{I}_M \mathbf{b} + \mathbf{n}', \tag{2.37}$$

where $\mathbf{I}_M$ denotes a $M \times M$ identity matrix and $\mathbf{c} = [c_1, \ldots, c_M]^T$, $\mathbf{n}' = \mathbf{H}^+\mathbf{n} = [n'_1, \cdots, n'_M]^T$ are the length M vectors.

In the L-Chase detector, inside each sub-detector, the noise term of the first detected j th symbol is

$$n'_{j,k} = c_j - \hat{b}_{j,k},\ k \in \{1, \cdots, q\}. \tag{2.38}$$

Assume that the index of other symbols is i and $i = 1, \cdots, j-1, j+1, \cdots, M$. The idea of the L-Chase detector is to estimate the noise term n'_i in (2.37) by using (2.38) and subtract the estimated n'_i from c_i. After that, better decision of the ith symbol could be made.

The decision of other symbols inside one sub-detector is

$$\hat{b}_{i,k} = dec\{c_i - p_{i,k} n'_{j,k}\} = dec\{c_i - p_{i,k}(c_j - \hat{b}_{j,k})\}, \tag{2.39}$$

where $p_{i,k}$ is the prediction coefficient. When $\hat{b}_{j,k}$ is correct, the noise variance of the ith symbol is

$$\begin{aligned}
&E[\left|n'_{i,k} - p_{i,k} n'_{j,k}\right|^2] \\
&= E[\left|\mathbf{w}_i \mathbf{n} - p_{i,k} \mathbf{w}_j \mathbf{n}\right|^2] \\
&= E[(\mathbf{w}_i \mathbf{n} - p_{i,k} \mathbf{w}_j \mathbf{n})(\mathbf{w}_i \mathbf{n} - p_{i,k} \mathbf{w}_j \mathbf{n})^H] \\
&= E[(\mathbf{w}_i - p_{i,k} \mathbf{w}_j)\mathbf{n}\mathbf{n}^H (\mathbf{w}_i - p_{i,k} \mathbf{w}_j)^H] \\
&= (\mathbf{w}_i - p_{i,k} \mathbf{w}_j)\sigma^2 \mathbf{I}_P (\mathbf{w}_i - p_{i,k} \mathbf{w}_j)^H \\
&= \sigma^2 \left\|\mathbf{w}_i - p_{i,k} \mathbf{w}_j\right\|^2,
\end{aligned} \tag{2.40}$$

where the P-length row vector $\mathbf{w}_i$ is the ith row of $\mathbf{H}^+$, the superscript H denotes Hermitian. When $p_{i,k}\mathbf{w}_j$ is the projection of $\mathbf{w}_i$ onto $\mathbf{w}_j$, the noise variance is minimized. Therefore the i th prediction coefficient is

$$p_{i,k} = \mathbf{w}_i \mathbf{w}_j^* / \left\| \mathbf{w}_j \right\|^2, \tag{2.41}$$

here, the notation "*" is the conjugate sign. Substitute (2.41) into (2.39), the hard decision values for other symbols within the kth sub-detector are

$$\hat{b}_{i,k} = dec\{c_i - \mathbf{w}_i \mathbf{w}_j^* (c_j - \hat{b}_{j,k}) / \left\| \mathbf{w}_j \right\|^2\}. \tag{2.42}$$

2.4 Summary

In this chapter, multiuser detection, the Chase algorithm and MIMO communication systems are reviewed. Among the presented well-known multiuser detectors, the multistage PIC detector is a good candidate for real-world implementation because it has less processing delay than the SIC detector and involves a simpler structure compared to the linear detectors. In Chapter 3, further research is carried out for multistage PIC detector. The Chase algorithm was originally proposed for decoding of block codes. This algorithm takes advantage of the channel measurement information and has the ability to correct the error of the less reliable symbols. In the rest of my thesis, the application of the Chase algorithm will be studied further. In MIMO systems, V-BLAST and two Chase based detectors for enhancing the performance of V-BLAST were introduced.

CHAPTER 3

CHASE BASED MULTISTAGE PIC DETECTORS

3.1 Introduction

As mentioned in Chapter two, *multiuser detection* (MUD) is an effective technique to mitigate *multiple access interference* (MAI) and ameliorate the performance of *direct-sequence code division multiple access* (DS-CDMA) systems. The optimum detector obtained superior performance improvement over conventional *matched filters* (MFs) detector, but its application was prohibited by the exponential complexity. Among the sub-optimum detectors which were proposed to alleviate the complexity, the multistage *parallel interference cancellation* (PIC) detector is a good candidate for the real-world implementation due to the fact that it has shorter processing delay than SIC and simpler structure than the linear detectors.

A key issue in multistage PIC scheme is to improve the hard decision accuracy after MFs. This objective basically can be achieved in two ways: One method is to keep the hard decision values after MFs intact and focuses on choosing the suitable weight for

each user in current stage such that the interference can be cancelled and the hard decision accuracy be improved in the next stage as much as possible. So far, most PIC schemes including partial PIC [23] and adaptive *normalized least-mean-square* PIC (NLMS-PIC) [11] belong to this class. Another method focuses on optimizing the hard decision values in current stage. Rather than directly using the hard decision values after MFs to do the interference cancellation, this approach reviews the possible hard decision combinations and selects the one minimizing a cost function as the final hard decision result to do the interference cancellation. The conventional optimum detector [3, 33] that considers all possible hard decision combinations at the expense of exponentially high complexity is one typical scheme in this class. However, in the second PIC scheme, it is not necessary to try all the hard decision combinations of all active users since the hard decision values after MFs do not have the same reliability. Using the Chase algorithm [10], we can keep the hard decision values with high reliabilities intact but try different hard decision combinations for the least reliable user data, and then select the final hard decision values based on a smaller set. In this chapter, a new multistage PIC scheme using NLMS algorithm in the earlier stages and the Chase algorithm in the later stages is proposed, which can achieve a better performance than multistage NLMS-PIC but with lower complexity. Our discussions are based on synchronous and asynchronous Rayleigh fading channels. For synchronous situation, we first introduce the model of Chase-PIC. And then, performance and complexity comparisons are executed among Chase-PIC, NLMS-PIC and their variants. After that, we make a conclusion that the proposed scheme can achieve better trade-off between performance and complexity compared to others. Subsequently, the proposed scheme is extended to asynchronous situation.

This chapter is organized as follows. In Section 3.2, we will discuss the Chase based multistage PIC detectors over synchronous channels. The application of Chase based multistage PIC detector over asynchronous channels is demonstrated in Section 3.3 and a summary is shown in Section 3.4.

3.2 Chase Based Multistage PIC Detectors over Synchronous Channels

As mentioned at the beginning of this chapter, the partial PIC and NLMS-PIC schemes could be considered as one category, which keeps the hard decision values after MFs intact and focuses on choosing the suitable weight for each user in current stage such that the interference can be cancelled and the hard decision accuracy be improved in the next stage as much as possible. In this section, We will discuss a new approach of PIC detector. Rather than directly using the hard decision values after MFs to do the interference cancellation, this approach uses the Chase algorithm to review the possible hard decision combinations and select the one minimizing a cost function as the final hard decision result to do the interference cancellation. A new multistage PIC scheme using NLMS algorithm in the earlier stages and the Chase algorithm in the later stages is proposed, which can achieve a better performance than multistage NLMS-PIC but with lower complexity. For explaining why this scheme is adopted, we first introduce the system model and Chase-PIC, and then performance and complexity comparisons are executed among Chase-PIC, NLMS-PIC and their variants. After that, we make a

conclusion that the proposed scheme can achieve a better trade-off between performance and complexity compared to others.

3.2.1 Synchronous System Model

Consider a synchronous DS-CDMA system in which K users communicate with the same rate over an uncorrelated flat Rayleigh fading channels corrupted by *additive white Gaussian noise* (AWGN). *Binary phase-shift keying* (BPSK) modulation is assumed for each user bit. The baseband received signal can be written as

$$r(t) = \sum_{i=1}^{K} s_i(t) + z(t)$$

$$= \sum_{i=1}^{K} A_i a_i c_i(t) + z(t). \tag{3.1}$$

If we consider sampling the continuous received signal at the chip rate N, (3.1) can be rewritten as

$$r(m) = \sum_{i=1}^{K} A_i a_i c_i(m) + z(m). \tag{3.2}$$

Here, A_i is a complex variable whose real and imaginary components are independent Gaussian random variables with zero-mean and variance 0.5 respectively. a_i is the ith user's data bit and $a_i \in \{1,-1\}$. $c_i(t)$ is the signature waveform and its amplitude $c_i(m) \in \{1/\sqrt{N}, -1/\sqrt{N}\}$, where N is the processing gain. $z(t)$ is a complex AWGN with zero-mean and two-sided power spectral density (PSD) of $N_0/2$ watts per hertz for each of the real and imaginary parts. Assuming perfect synchronization, after the conventional matched filter bank, the output can be written as

$$y_i = \int_0^{Tb} r(t)A_i^* c_i^*(t)dt$$

$$= \int_0^{Tb} [\sum_{j=1}^{K} A_j a_j c_j(t) + z(t)]A_i^* c_i^*(t)dt$$

$$= |A_i|^2 a_i + \sum_{\substack{j=1 \\ j\neq i}}^{K} A_j A_i^* a_j \rho_{j,i} + n_i , \tag{3.3}$$

where the notation "*" is the conjugate sign, $\rho_{j,i}$ is a correlation coefficient and n_i is the noise term after dispreading. $\rho_{j,i}$ and n_i are expressed as

$$\rho_{j,i} = \int_0^{Tb} c_j(t)c_i^*(t)dt$$

$$= \sum_{m=0}^{N-1} c_j(m)c_i^*(m), \tag{3.4}$$

and

$$n_i = \int_0^{Tb} z(t)A_i^* c_i^*(t)dt$$

$$= \sum_{m=0}^{N-1} z(m)A_i^* c_i^*(m). \tag{3.5}$$

The right-hand side of (3.3) consists of three parts: the desired signal $|A_i|^2 a_i$, *multiple access interference* (MAI) $\sum_{\substack{j=1 \\ j\neq i}}^{K} A_j A_i^* a_j \rho_{j,i}$ and the noise n_i. The conventional single-user detector treats MAI as another noise and the estimated data $\hat{a}_i$ for a_i is

$$\hat{a}_i = \text{sgn}\{\text{Re}\{y_i\}\}. \tag{3.6}$$

3.2.2 Multistage Chase-PIC Detector

For a K-user synchronous CDMA system, the output of the optimum detector is the vector $\hat{\mathbf{a}} = [\hat{a}_1, \ldots, \hat{a}_K]^T$ that minimizes the cost function [3], [33].

$$\varepsilon = \int_0^{Tb} \left| r(t) - \sum_{i=1}^{K} A_i \hat{a}_i c_i(t) \right|^2 dt \tag{3.7}$$

Assuming the received signal is sampled at the chip rate after chip-matched filtering, the cost function (3.7) can be rewritten as

$$\sum_{m=0}^{N-1} \left| r(m) - \sum_{i=1}^{K} A_i c_i(m) \hat{a}_{i,j} \right|^2 \qquad j \in \{1, 2, 3, \cdots, 2^n\}, \tag{3.8}$$

here, n is the number of users whose data is not known to the detector. The optimum detector finds the solution by exhaustive search, i.e. by letting n=K, calculating (3.8) for 2^K possible bit patterns and choosing the one that minimizes this function. This approach results in exponential complexity with respect to the number of user K.

This high complexity can be reduced by using Chase algorithm [10] which is used for decoding block codes with channel measurement information. The principle in Chase decoder can be used in a PIC multiuser detector. After the single-user MFs, the reliabilities of hard decisions are not identical. So, we can consider both alternatives (1 and -1) for the n least reliable hard decisions but keep the other K-n more reliable hard decision values. From this smaller set of 2^n patterns, we can select the one that minimizes (3.8) as the final hard decision and then do parallel interference cancellation. This method is defined as Chase-PIC and can be extended to multistage situation. The diagram of two-stage Chase-PIC is illustrated in Fig. 3.1, and the block deciding hard

decision $\hat{\mathbf{a}} = [\hat{a}_1, \ldots, \hat{a}_K]^T$ with the Chase algorithm and doing interference cancellation is shown in Fig. 3.2.

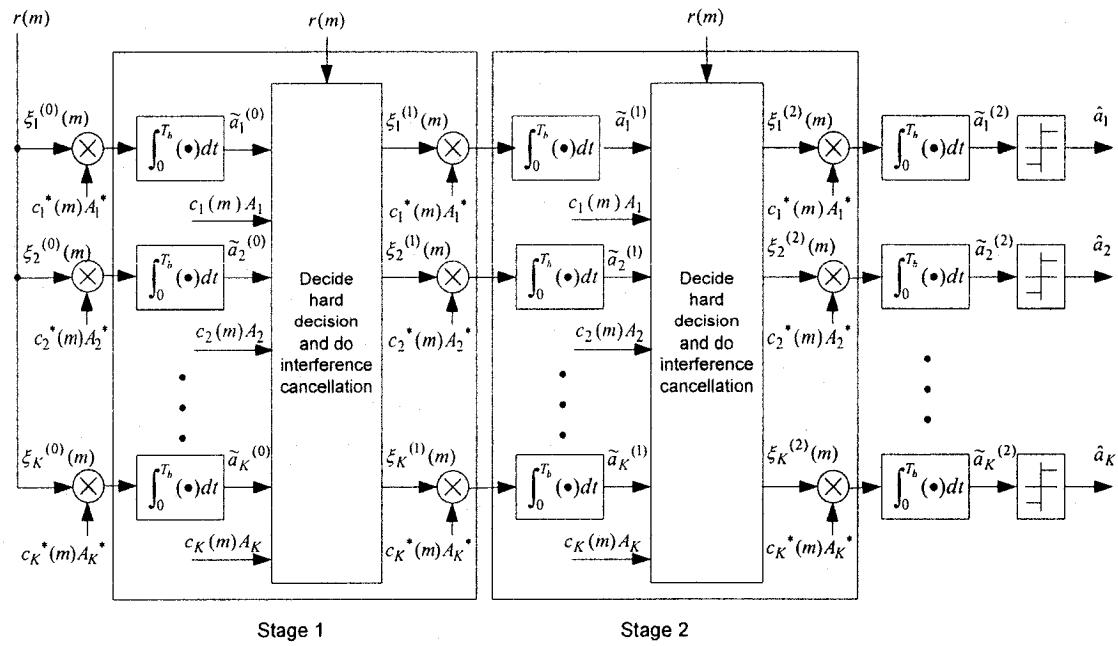

Figure 3.1 Two stages Chase-PIC block diagram over synchronous channels

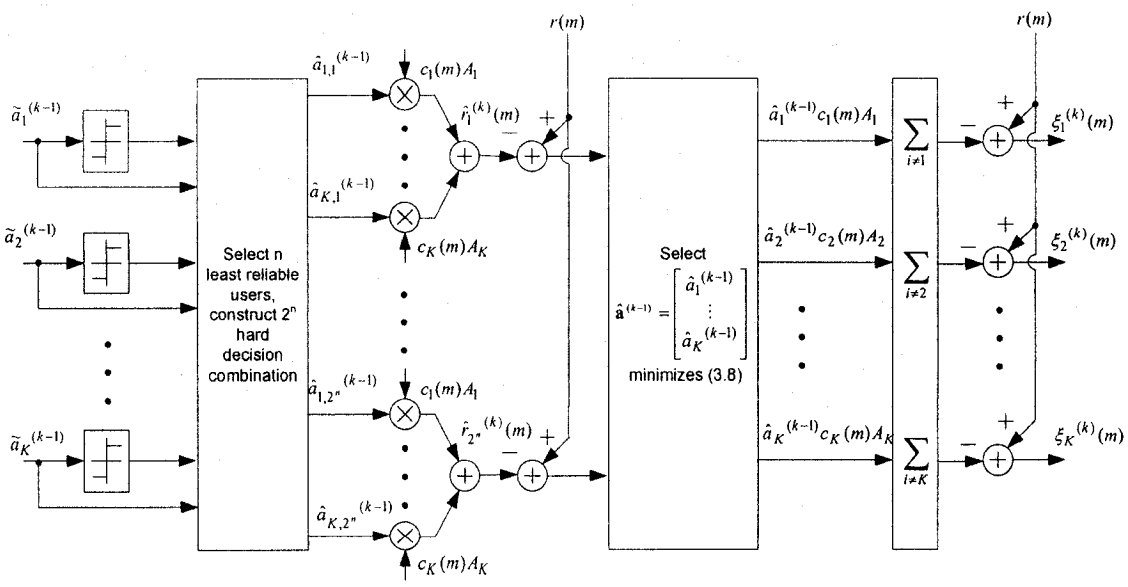

Figure 3.2 Hard decision value selection using the Chase algorithm and interference cancellation over synchronous channels

Our discussion is based on the condition that the continuous received signal is sampled at the chip rate $R_c = NR_b$, where R_b is the bit rate, and the procedure inside one stage Chase-PIC is illustrated below:

Step 1: Calculate the soft decision values after MFs.

$$\tilde{a}_i^{(k-1)} = \sum_{m=1}^{N} \xi_i^{(k-1)}(m) A_i^* c_i^*(m) \qquad i \in \{1,2,\cdots,K\}, \tag{3.9}$$

here, $\xi_i^{(k-1)}(m)$ is the chip information of user i after interference cancellation in stage k-1. When k-1=0, $\xi_i^{(k-1)}(m) = r(m)$.

Step 2: Select n least reliable users and construct 2^n hard decision combinations.

The selection of the number n can be based on the performance of the conventional single-user MFs detector. The n users with smallest absolute values of the real part of $\tilde{a}_i^{(k-1)}$ are the least reliable users. The possible hard decisions are the vectors $\hat{\mathbf{a}}_j^{(k-1)} = [\hat{a}_{1,j}^{(k-1)}, \ldots, \hat{a}_{1,j}^{(k-1)}]^T$, $j \in \{1,2,3,\cdots,2^n\}$.

Step 3: Respread and estimate the received signals.

The estimate of the received signals in this step can be written as

$$\hat{r}_j^{(k)}(m) = \sum_{i=1}^{K} A_i \hat{a}_{i,j}^{(k-1)} c_i(m), \quad j \in \{1,2,3,\cdots,2^n\}. \tag{3.10}$$

Step 4: Select the final hard decision $\hat{\mathbf{a}}^{(k-1)} = [\hat{a}_1^{(k-1)}, \ldots, \hat{a}_K^{(k-1)}]^T$ by minimizing the cost function (3.8).

Step 5: Interference cancellation

$$\xi_i^{(k)}(m) = r(m) - \sum_{\substack{j=1 \\ j \neq i}}^{K} A_j \hat{a}_j^{(k-1)} c_j(m). \tag{3.11}$$

The interference cancellation results $\xi_i^{(k)}(m)$ are multiplied by $c_i^*(m)A_i^*$ and then sent to the next stage.

The one stage computational complexity comparison between Chase-PIC and NLMS-PIC [11] is displayed in Table 3.1 and 3.2. The complexity computation is carried out from the soft output of single-user MFs $\tilde{a}_i^{(k-1)}$ to getting $\xi_i^{(k)}(m)$ after interference cancellation. The formulas calculating NLMS-PIC are taken from the reference [11].

Operation / Steps	Multiplication	Add/Subtraction	Absolute	Comparison
After MFs, find possible error user location	0	0	K	$n{\cdot}K$
Decide possible hard decision set	0	0	0	K
(3.10)	$3(K\text{-}n)N$ $+3{\cdot}2^n{\cdot}N$	0	0	0
$r(m)-\sum_{i=1}^{K} r_i^{(k)}(m)$	0	$2[(K\text{-}1\text{-}n)N$ $+2^n{\cdot}n{\cdot}N+2^n{\cdot}N]$	0	0
Minimizing (3.8)	$4{\cdot}2^n{\cdot}N$	$2^n(N\text{-}1)$	0	2^n
(3.11)	0	$2K{\cdot}N$	0	0
Total	$3(K\text{-}n)N$ $+7{\cdot}2^n{\cdot}N$	$2N(3K\text{-}n\text{-}1)$ $+2^n(2n{\cdot}N+3N\text{-}1)$	K	$(n+1)K+2^n$

Table 3.1 One stage Chase-PIC complexity computation over synchronous channels (K active users)

Operations / Steps	Multiplication	Add/Subtraction	Comparison
Hard decision	0	0	K
$s_i^{(k)}(m) = c_i(m)\hat{a}_i^{(k-1)}$	$K{\cdot}N$	0	0
$\hat{r}^{(k)}(m) = \sum_{i=1}^{K} s_i^{(k)}(m)\lambda_i^{(k)}(m)$	$2K{\cdot}N$	$2(K\text{-}1)N$	0
$e^{(k)}(m) = r(m) - \hat{r}^{(k)}(m)$	0	$2N$	0
$\left\|\hat{\mathbf{s}}^{(k)}(m)\right\|^2$	$K{\cdot}N$	$(K\text{-}1)\cdot N$	0
$\boldsymbol{\lambda}^{(k)}(m+1) = \boldsymbol{\lambda}^{(k)}(m) + \frac{\mu}{\left\|\hat{\mathbf{s}}^{(k)}(m)\right\|^2}\left[\hat{\mathbf{s}}^{(k)}(m)\right]^* e^{(k)}(m)$	$2(K{+}2)N$	$2K{\cdot}N$	0
$\xi_i^{(k)}(m) = r(m) - \sum_{\substack{j=1 \\ j\neq i}}^{K} \lambda_j^{(k)}(N-1)\hat{s}_j^k(m)$	$2K{\cdot}N$	$2K{\cdot}N$	0
Total	$8K{\cdot}N{+}4N$	$7K{\cdot}N{-}N$	K

Table 3.2 One stage NLMS-PIC complexity computation over synchronous channels (*K* active users)

Number of Active User K	Number of erroneous bits n			
	Mode 1	Mode 2	Mode 3	Mode 4
1	0	0	0	0
5	1	2	1	1
10	2	3	1	1
15	3	4	1	1
20	3	4	1	1
25	4	5	2	1
30	4	5	2	1

Table 3.3 The mode list of possible error user number

	Multiplication	Add/Subtraction	Absolute	Comparison
NLMS-PIC	244N	209N	0	30
Chase-PIC (mod 1)	190N	346N-16	30	166
Chase-PIC (mod 2)	299N	484N-32	30	212
Chase-PIC (mod 3)	112N	202N-4	30	94
Chase-PIC (mod 4)	101N	186N-2	30	62
Chase(mod 4)-NLMS-PIC	434N	495N-16	30	196

Table 3.4 The complexity comparison of different schemes over synchronous channels (30 active users)

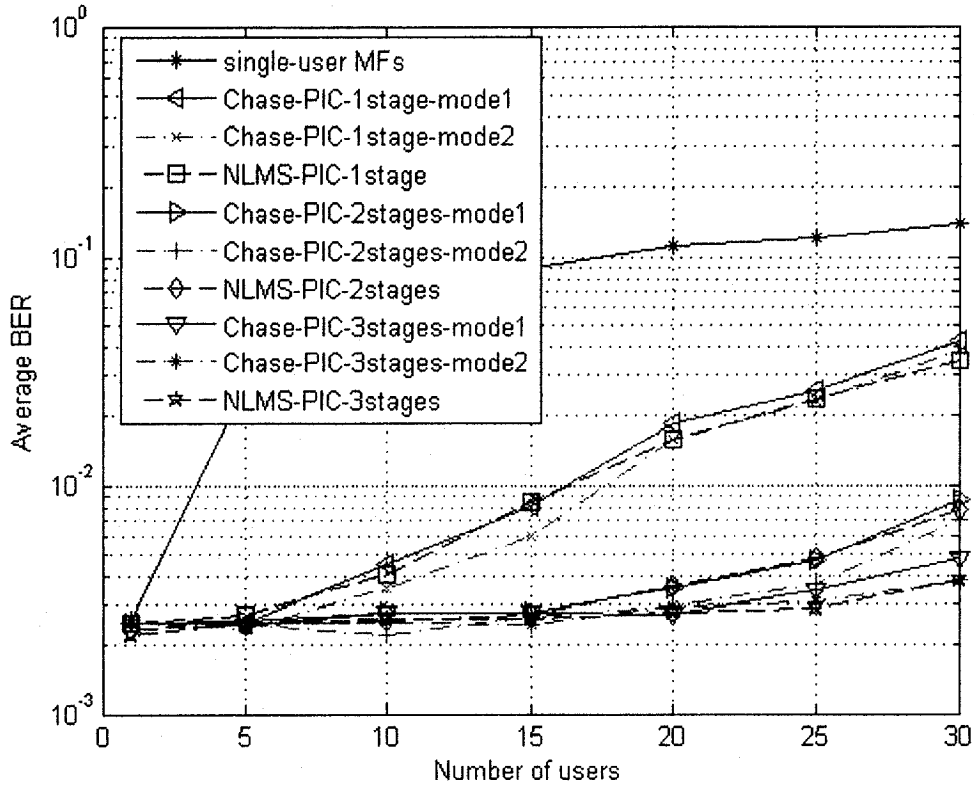

Figure 3.3 Performance comparison over synchronous channels : Chase-PIC vs. NLMS-PIC (E_b / N_o=20dB, processing gain N=32)

Fig. 3.3 compares the performances of 1, 2, 3 stages Chase-PIC and NLMS-PIC. The step sizes for 1st, 2nd, and 3rd stage NLMS-PIC are 0.2, 0.03, and 0.01 respectively. Information bits are spread using randomly generated scrambling sequences with a processing gain of N=32. Perfect channel estimation is assumed. In this thesis, we focus on the multiuser interference cancellation, so signal noise ration (SNR) E_b / N_o assumed to be 20dB. The mod 1, 2, 3, 4 mean the different possible error user number models which are listed in Table 3.3. The complexity comparison among different

schemes for 30 active users is shown in Table 3.4. The Chase-NLMS-PIC scheme in this table will be discussed in Subsection 3.2.3.

In Fig. 3.3, the performance of the conventional single-user detector is also shown as a baseline for comparison. This figure shows that the performance of the Chase-PIC detector can be improved if we increase the number of users that are assumed to be unreliable. For 30 active users, from Fig. 3.3 and Table 3.4, we observe that Chase-PIC (mode 2) achieves similar performance as NLMS-PIC with little increase in complexity. The problem of Chase-PIC is that its complexity is exponential with the number of selected users even though it can significantly decrease the complexity compared to the optimum detector,. When the number of active users is high, we have to increase the number on unreliable user bits in order to obtain a certain performance. This, in turn, increases the complexity. Therefore, using only Chase algorithm in multistage PIC is not good enough for a real life implementation compared to some previous developed schemes like NLMS-PIC.

3.2.3 Multistage Chase-NLMS-PIC Detector

In this section, we discuss the complexity and performance of the Chase-NLMS-PIC detector which combines the Chase and NLMS algorithms. In each stage, this detector first uses estimated channel gains and the Chase algorithm to decide hard decision data; furthermore, the coefficients for each hard decision data are optimized by NLMS; finally, interference cancellation is carried out.

The performance comparison between the Chase-NLMS-PIC scheme and the NLMS-PIC scheme is shown in Fig. 3.4. With two optimal techniques, the system performance is enhanced. The two-stage Chase-NLMS-PIC scheme can achieve almost the same performance as three-stage NLMS-PIC scheme but unfortunately the complexity of two-stage Chase-NLMS-PIC is higher than three-stage NLMS-PIC (Table 3.4).

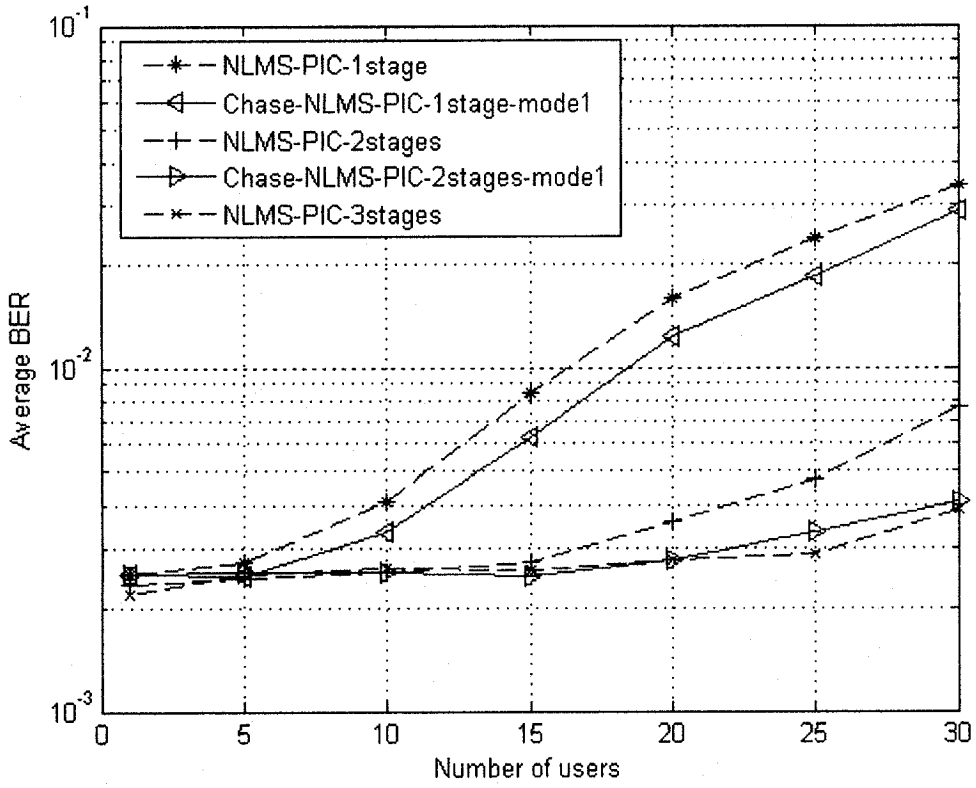

Figure 3.4 Performance comparison over synchronous channels: Chase-NLMS-PIC vs. NLMS-PIC (E_b / N_o =20dB, processing gain N =32)

3.2.4 Proposed Multistage Chase Based PIC Detector

In general, the number of unreliable bits selected is inversely proportional to the hard decision accuracy after MFs. This means that if the hard decision accuracy is high, we can choose smaller number of user bits for reconsideration. On the other hand, we have to choose more bits when the hard decision accuracy is low. So a better multistage PIC scheme would be like this: in the earlier stages where the hard decision accuracy is low, we employ NLMS-PIC scheme; in the later stages where the hard decision accuracy has improved, we can use the Chase-PIC scheme. Fig. 3.5 displays the performance using the NLMS algorithm in the first stage and the Chase algorithm in other stages. From table 3.4 and Fig. 3.5, Using mode 3, 4 of the possible error user number in the second stage and mode 4 of the possible error user number in the third stage, we can obtain better performance than two-stage and three-stage NLMS-PIC but with less complexity.

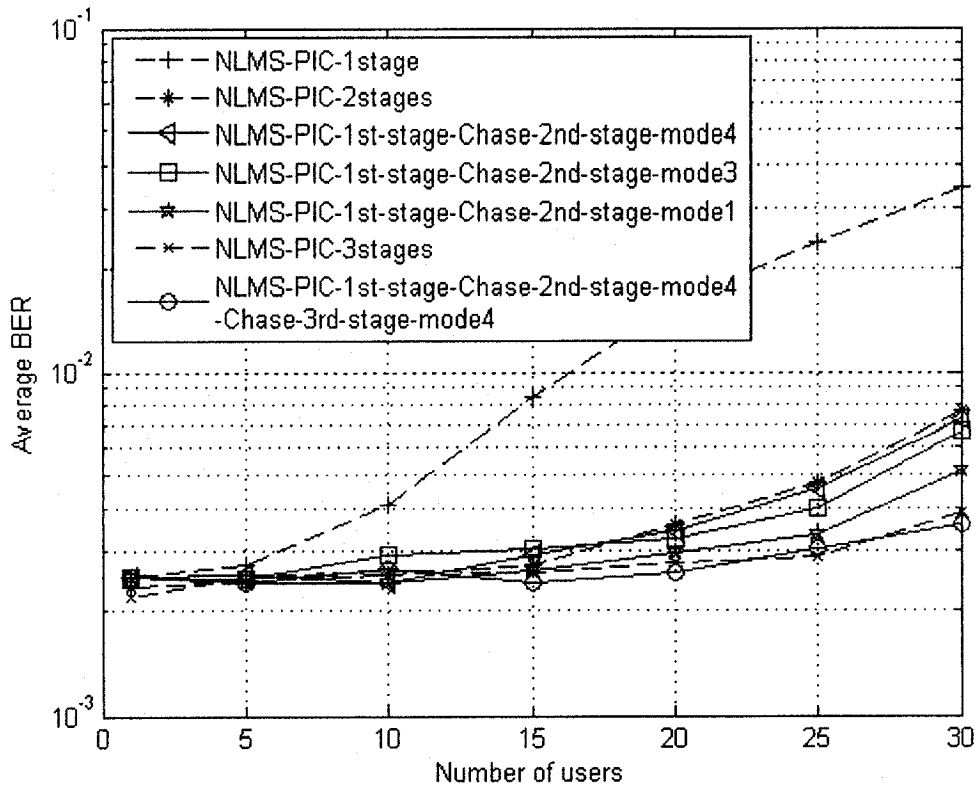

Figure 3.5 Performance comparison over synchronous channels: the proposed scheme vs. NLMS-PIC (E_b / N_o =20dB, processing gain N =32)

3.3 Chase Based Multistage PIC Detector over Asynchronous Channels

The discussion of the Chase based multistage PIC scheme over synchronous Rayleigh fading channels was presented in Subsection 3.2.4, which proposed a new multistage PIC scheme using the NLMS algorithm in the earlier stages and the Chase algorithm in the later stages. In this section, the proposed scheme is extended to asynchronous channels. The simulation results show that the advantage achieved using the proposed scheme over

synchronous channels is still kept, i.e., it has a better performance compared to multistage NLMS-PIC but with complexity reduction.

3.3.1 Asynchronous System Model

Consider a K users asynchronous CDMA system using BPSK modulation over an uncorrelated frequency-selective Rayleigh fading channel corrupted by AWGN. For L resolvable paths, the baseband received signal can be written as

$$r(t) = \sum_{l=1}^{L} \sum_{i=1}^{K} s_i(t - \tau_{i,l}) + z(t)$$

$$= \sum_{l=1}^{L} \sum_{i=1}^{K} A_{i,l} a_i c_i(t - \tau_{i,l}) + z(t). \tag{3.12}$$

The discrete form of (3.12) can be obtained by sampling the continuous received signal at the chip rate N and written as

$$r(m) = \sum_{l=1}^{L} \sum_{i=1}^{K} A_{i,l} a_i c_i(m - m_{i,l}) + z(m), \tag{3.13}$$

here, $A_{i,l}$, the Rayleigh fading channel coefficient of the ith user in the lth resolvable path, is a complex variable whose real and imaginary components are independent Gaussian random variables with zero-mean and variance $0.5/L$ respectively and its value doesn't change within a bit interval; a_i is the ith user's data bit and $a_i \in \{1,-1\}$; $c_i(t)$ is the signature waveform and its amplitude $c_i(m) \in \{1/\sqrt{N}, -1/\sqrt{N}\}$, where N is the processing gain; $\tau_{i,l}$ denotes the relative delay of the ith user in the lth path and $\tau_{i,l} = m_{i,l} T_c$, where T_c is the chip interval; $z(t)$ is a complex AWGN with zero-mean and

two-sided power spectral density (PSD) of $N_0/2$ watts per hertz for each of the real and imaginary parts.

For the ith user, the output at each finger of RAKE receiver is

$$y_{i,l} = \int_{\tau_{i,l}}^{T_b+\tau_{i,l}} r(t)\, c_i^{*}(t-\tau_{i,l})dt$$

$$= \sum_{m=0}^{N-1} r(m)\, c_i^{*}(m - m_{i,l}), \tag{3.14}$$

where "*" is the conjugate sign. Using maximal ratio combining rule [14], the combining outputs of these fingers are

$$y_i = \sum_{l=1}^{L} A_{i,l}^{*}\, y_{i,l}. \tag{3.15}$$

The estimated data $\hat{a}_i$ for a_i after the conventional single-user RAKE receiver is written as

$$\hat{a}_i = \mathrm{sgn}\{\mathrm{Re}\{y_i\}\}. \tag{3.16}$$

3.3.2 Proposed Multistage Chase Based PIC Detector over Asynchronous Channels

In this section, the proposed multistage PIC scheme that adopts the NLMS algorithm in the earlier stages and the Chase algorithm in the later stages over asynchronous channels is demonstrated. If we know the Chase-PIC scheme, its combination with NLMS-PIC as the proposed scheme is just straight forward. Therefore, at the beginning, the Chase-PIC model over asynchronous channels is presented. And then, the complexity and performance comparisons between the proposed scheme and NLMS-PIC will be

illustrated. Simulation and complexity calculation show that the proposed scheme can also achieve better performance over an asynchronous channel compared to multistage NLMS-PIC but with less complexity.

In asynchronous channels, the cost function (3.8) can be modified as

$$\sum_{m=m_0}^{m_d} \left| r(m) - \sum_{l=1}^{L} \sum_{i=1}^{K} A_{i,l} c_i (m - m_{i,l}) \hat{a}_{i,j} \right|^2 . \tag{3.17}$$

The range of m in (3.17) is the same transmitted symbol overlap over different path. The diagram of one stage Chase-PIC is illustrated in Fig. 3.6, and the block deciding hard decision $\hat{\mathbf{a}} = [\hat{a}_1, \ldots, \hat{a}_K]^T$ with the Chase algorithm and doing interference cancellation is shown in Fig. 3.7.

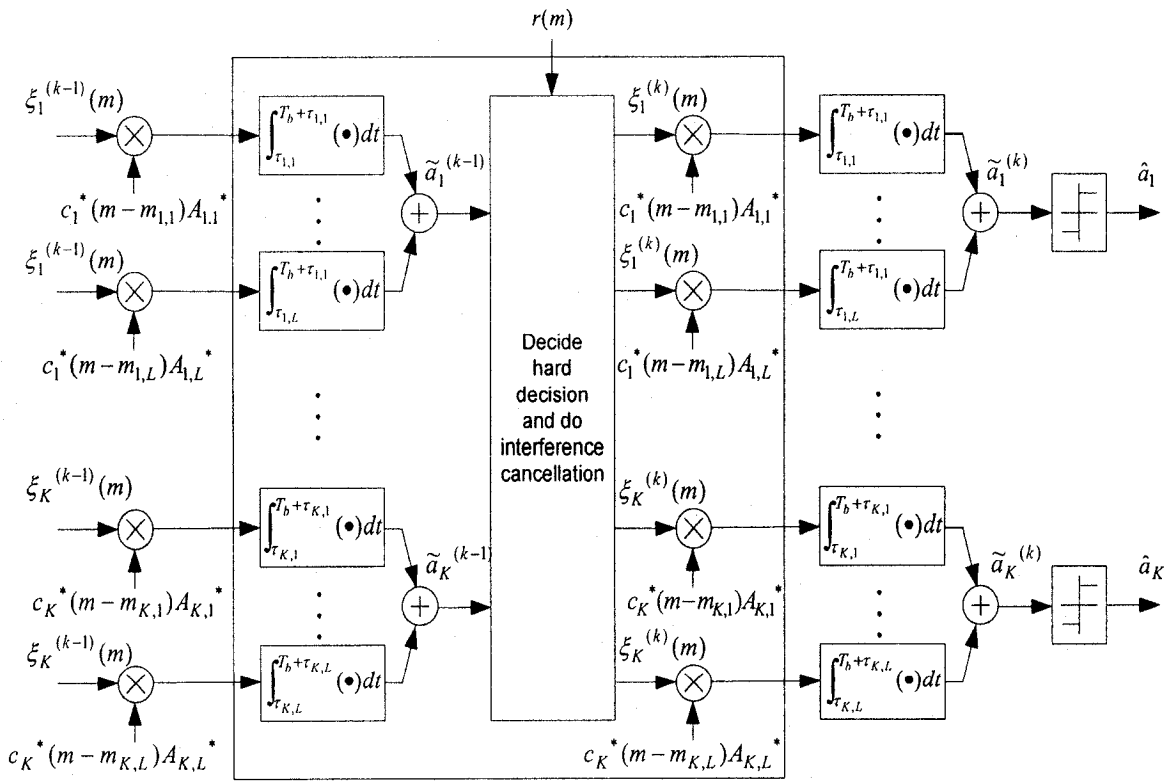

Figure 3.6 One stage Chase-PIC block diagram over asynchronous channels

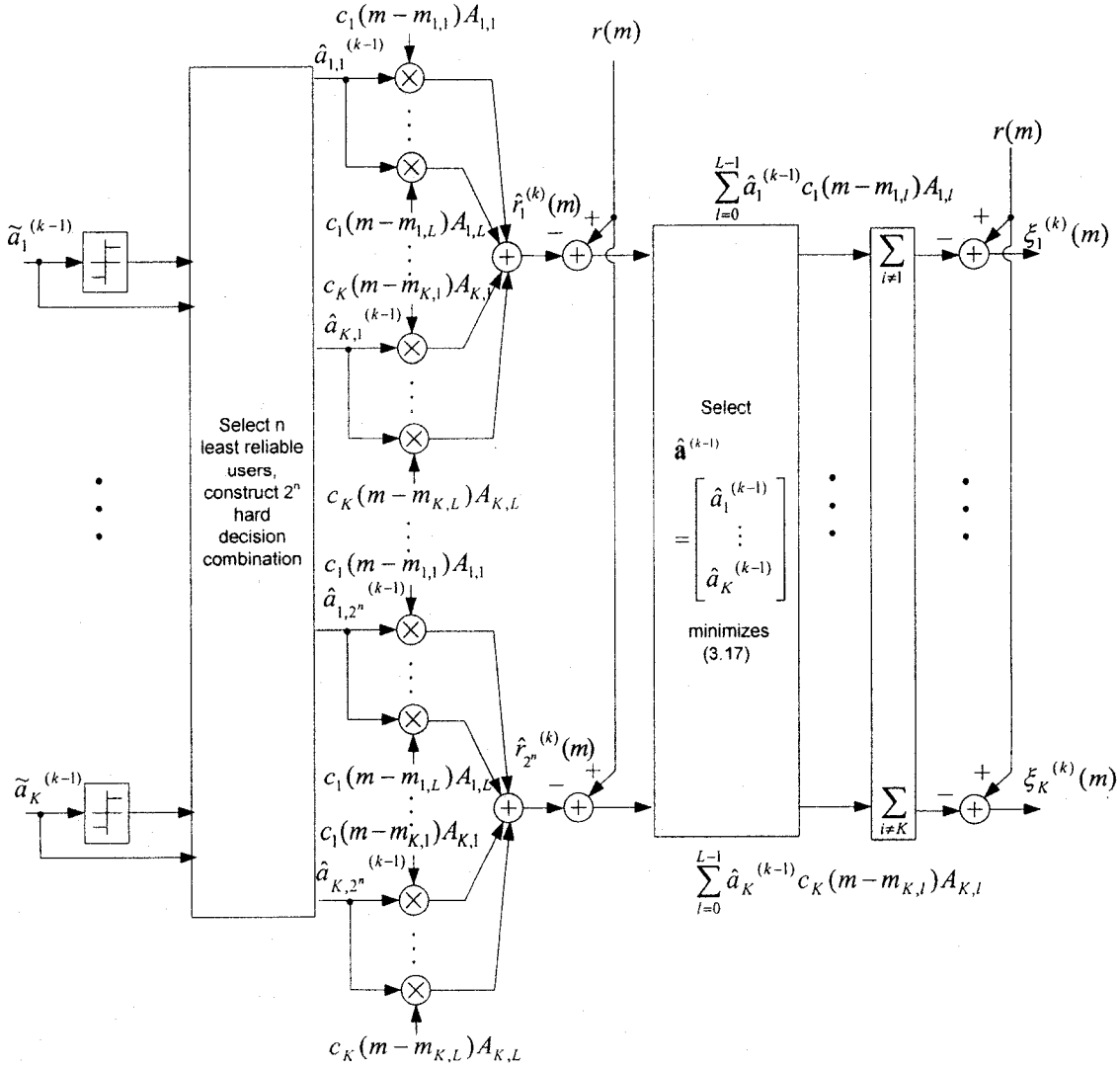

Figure 3.7 Hard decision value selection using the Chase algorithm and interference cancellation over asynchronous channels

Similar to synchronous channels, the procedure inside one stage Chase-PIC is illustrated below:

Step 1: Calculate the soft decision values after MFs.

$$\tilde{a}_i^{(k-1)} = \sum_{l=1}^{L} \sum_{m=0}^{N-1} \xi_i^{(k-1)}(m) A_{i,l}^{*} c_i^{*}(m - m_{i,l}) \quad i \in \{1,2,\cdots,K\}, \tag{3.18}$$

here, $\xi_i^{(k-1)}(m)$ is the chip information of user i after interference cancellation in stage $k-1$. When $k-1=0$, $\xi_i^{(k-1)}(m)=r(m)$.

Step 2: Select n least reliable users and construct 2^n hard decision combinations.

The selection of the number n is based on the performance of the conventional single-user RAKE detector. The n users with smallest absolute values of the real part of $\tilde{a}_i^{(k-1)}$ are the least reliable users. The possible hard decisions are the vectors $\hat{\mathbf{a}}_j^{(k-1)}=[\hat{a}_{1,j}^{(k-1)},\ldots,\hat{a}_{K,j}^{(k-1)}]^T$, $j\in\{1,2,3,\cdots,2^n\}$.

Step 3: Respread and estimate the received signals.

The estimate of the received signals in this step can be written as

$$\hat{r}_j^{(k)}(m)=\sum_{l=1}^{L}\sum_{i=1}^{K}A_{i,l}\hat{a}_{i,j}^{(k-1)}c_i(m-m_{i,l}) \quad j\in\{1,2,3,\cdots,2^n\}. \tag{3.19}$$

Step 4: Select final hard decision $\hat{\mathbf{a}}^{(k-1)}=[\hat{a}_1^{(k-1)},\ldots,\hat{a}_K^{(k-1)}]^T$ minimizing the cost function (3.17).

Step 5: Interference cancellation

$$\xi_i^{(k)}(m)=r(m)-\sum_{l=1}^{L}\sum_{\substack{j=1\\ j\neq i}}^{K}A_{j,l}\hat{a}_j^{(k-1)}c_j(m-m_{j,l}). \tag{3.20}$$

The interference cancellation results $\xi_i^{(k)}(m)$ are passed into RAKE receiver and then the hard decision values are sent to the next stage.

As discussed in Subsection 3.2.4, for achieving certain performance, the number of unreliable bits selected is inversely proportional to the hard decision accuracy after MFs. The more unreliable bits we select, the better performance we can obtain and the trade-

off is the exponential increase in complexity. If there are a large number of active users and Chase-PIC is applied in the earlier stage, its complexity is higher than NLMS-PIC due to the low decision accuracy after MFs. But in the later stages, the complexity of Chase-PIC is lower than NLMS-PIC for achieving the same performance due to the high hard decision accuracy after MFs. So a multistage PIC scheme, which can make use of the advantages of NLMS-PIC and Chase-PIC, would be like this: in the earlier stages when the hard decision accuracy is low we employ the NLMS-PIC scheme; in the later stages when the hard decision accuracy has improved we can use the Chase-PIC scheme.

For simplicity, the comparison between the proposed scheme and NLMS-PIC is carried on a case with two stages. In the proposed scheme, the first stage utilizes NLMS-PIC and the second stage adopts Chase-PIC. Two resolvable paths are considered in this section and the time delay of the second path is one chip interval T_c. The complexity (30 active users) and performance comparisons of multistage NLMS-PIC and the proposed scheme over asynchronous Rayleigh fading channel are shown in Table 3.5 and Fig. 3.8. The complexity computation is carried out from soft output of single-user MFs $\tilde{a}_i^{(k-1)}$ to getting $\xi_i^{(k)}(m)$ after interference cancellation. The complexity calculation of NLMS-PIC is based on the reference [11]. From these comparisons, we know the proposed scheme can obtain better performance than multistage NLMS-PIC but with less complexity. Here, the step sizes for 1st, 2nd stage NLMS-PIC are 0.2 and 0.03. Information bits are spread using randomly generated scrambling sequences with a processing gain of $N = 32$. Perfect channel estimation and 20dB E_b / N_o are assumed.

The mode 3, 4 mean the different possible error user number modes that are listed in Table 3.3.

	Multiplication	Add/Subtraction	Comparison
NLMS-PIC	856*N*	86*N*	60
Proposed scheme (mode 4)	622*N*	169*N*-4	92
Proposed scheme (mode 3)	636*N*	185*N*-8	124

Table 3.5 The complexity comparison over asynchronous channels: proposed scheme vs. NLMS-PIC (30 active users)

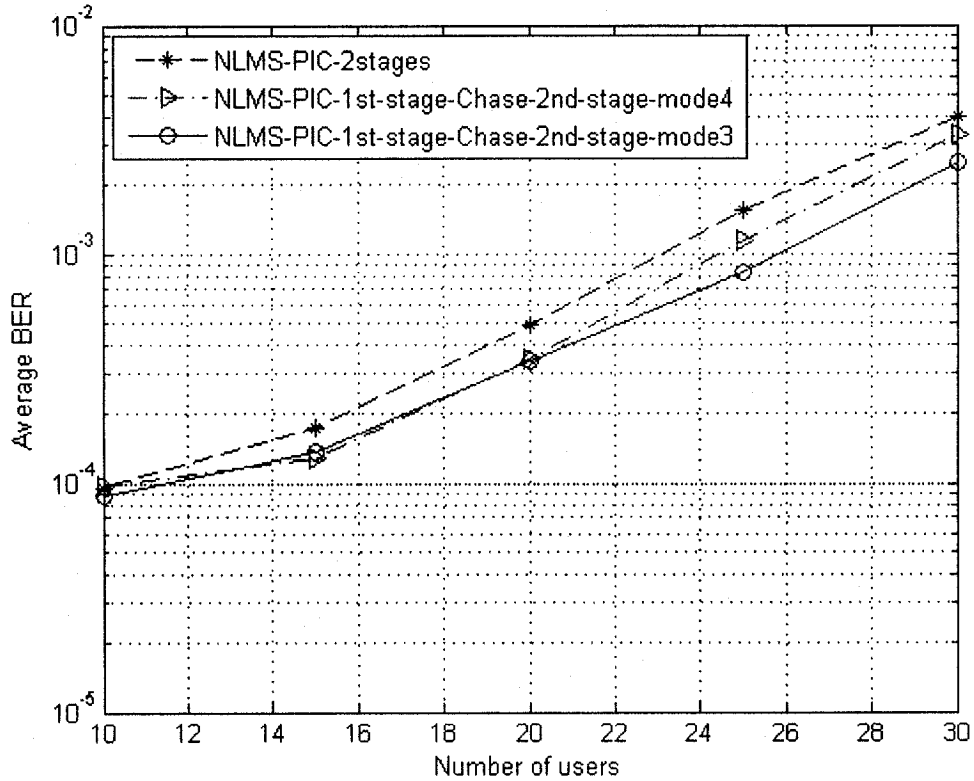

Figure 3.8 Performance comparison over asynchronous channels: proposed scheme vs. NLMS-PIC (E_b / N_o =20dB, processing gain N =32, 2 resolvable paths)

3.4 Summary

In this chapter, a new approach, which uses the Chase algorithm to optimize the hard decision accuracy, is used in the PIC detectors. After performance and complexity comparisons, a new PIC scheme that uses the NLMS algorithm in the earlier stages and the Chase algorithm at the later stages is proposed. Simulation and complexity calculation show that the proposed scheme can achieve better performance than multistage NLMS-PIC but with less complexity over synchronous and asynchronous channels.

CHAPTER 4

CHASE BASED MIMO-CDMA DTETECTORS

4.1 Introduction

For next generation wireless systems, there is an ever increasing demand for high data rate and improved reliability. This demand can be met by combining the time-domain technique of *multiuser detection* (MUD) [1] with a space-domain technique—the *vertical Bell Laboratories layered space-time* (V-BLAST) scheme [29]. The combination of these two techniques was developed in [34, 35], which proposed the *layered space-time multiuser detetor* (LAST-MUD) over the uplink of a *multiple-input multiple-output code division multiple access* (MIMO-CDMA) system.

In this chapter, the Chase algorithm is studied to improve the performance of LAST-MUD. First, we will introduce the MIMO-CDMA system model and LAST-MUD. After that, the B-Chase and L-Chase detectors, which were originally proposed in [12] for enhancing the performance of single user V-BLAST system, are discussed in MIMO-CDMA systems. Finally, after analysing the weakest detected symbol in LAST-MUD, a

new Chase based scheme is proposed. This proposed scheme has less complexity than the B-Chase detector and the simulation result shows that the proposed scheme can achieve a better performance compared to the B-Chase detector at high SNR.

4.2 System Model and Layered Space-Time Multiuser Detector

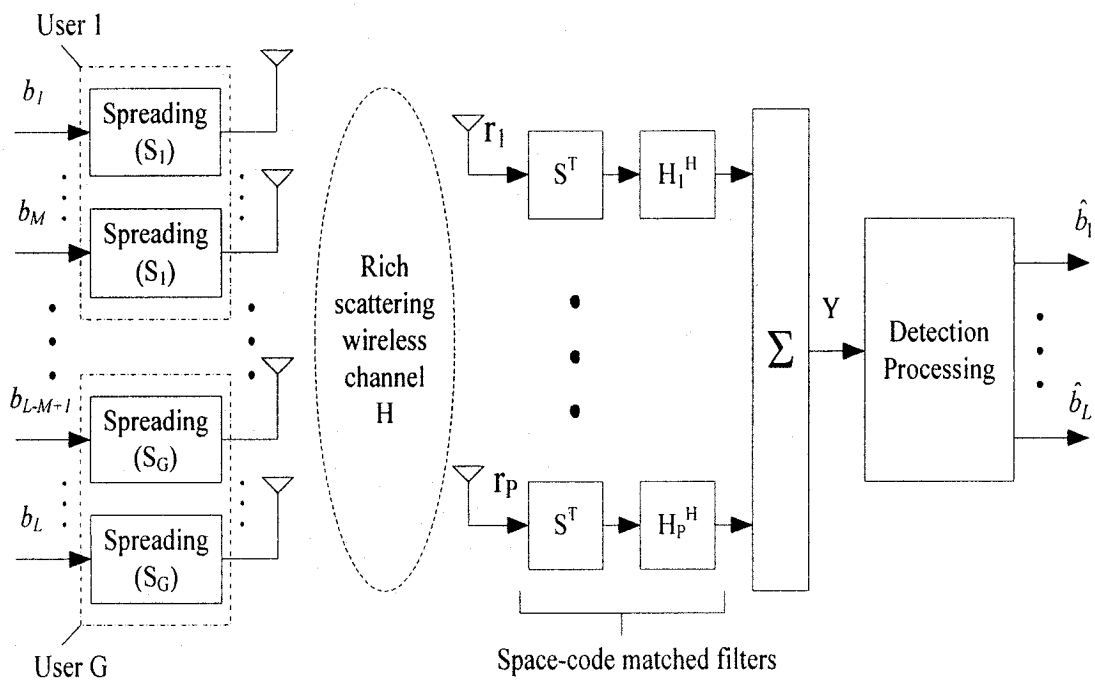

Figure 4.1 MIMO-CDMA Multiuser System Block Diagram

The configuration of a synchronous MIMO-CDMA system is shown in Fig. 4.1. In this system, there are G users each with M antennas. Each user has a separate spreading code and uses this code on all its M antennas. The total number of transmitter antennas in the system is $L = G \times M$. At the receiver, there are P receive antennas. The channels between transmitter and receiver are assumed to be uncorrelated flat Rayleigh fading.

The channel matrix is written as $\mathbf{H} = [\mathbf{h}_1, \cdots, \mathbf{h}_P]^T$, where $\mathbf{h}_p$ is the length L channel coefficient vector between the pth receive antenna and all L transmit antennas. The baseband received signal at the pth antenna can be written as

$$\mathbf{r}_p = \mathbf{S}\mathbf{H}_p\mathbf{b} + \mathbf{n}_p, \tag{4.1}$$

where $\mathbf{r}_p$ is a complex column vector of length N where N is the spreading factor. $\mathbf{S}$ is the $N \times L$ random spreading matrix and $\mathbf{S} = [\mathbf{S}_1, \ldots, \mathbf{S}_1, \mathbf{S}_2, \ldots, \mathbf{S}_2, \ldots, \mathbf{S}_G, \ldots, \mathbf{S}_G]$. The amplitude of each element in $\mathbf{S}$ is $1/\sqrt{N}$ or $-1/\sqrt{N}$. $\mathbf{H}_p$ denotes the $L \times L$ complex diagonal channel matrix and its diagonal elements are the entries of vector $\mathbf{h}_p$. The channel coefficient is a complex variable whose real and imaginary components are independent Gaussian random variables with zero-mean and variance 0.5 respectively. The vector $\mathbf{b} = [b_1, \ldots, b_L]^T$ is the length L symbol vector where each element represents the symbol transmitted from a single antenna. Here, QPSK modulation is assumed and the transmitted symbol is a complex variable whose real and imaginary components have magnitude $\sqrt{1/(M \times 2)}$ respectively. The noise is represented by $\mathbf{n}_p$, a complex-valued zero-mean Gaussian random vector of length N with the covariance matrix $\sigma^2\mathbf{I}_N$, where $\mathbf{I}_N$ denotes the $N \times N$ identity matrix.

At the receiver side, the space-code matched filters, which are matched to the spreading codes and the channel coefficients, are constructed. Let $\mathbf{Y}$ be the length L sufficient statistic vector obtained after the space-code matched filters and it can be written as

$$\mathbf{Y} = \sum_{p=1}^{P} \mathbf{H}_p^H \mathbf{S}^T \mathbf{r}_p = \mathbf{R}\mathbf{b} + \tilde{\mathbf{n}}, \tag{4.2}$$

here $\mathbf{R} = \sum_{p=1}^{P} \mathbf{X}_p^H \mathbf{X}_p$ is the $L \times L$ space-code cross-correlation matrix in which $\mathbf{X}_p = \mathbf{S}\mathbf{H}_p$ and $\tilde{\mathbf{n}} = \sum_{p=1}^{P} \mathbf{X}_p^H \mathbf{n}_p$ is the length L noise vector with the covariance matrix $\sigma^2 \mathbf{R}$.

The detection procedure of LAST-MUD is similar to V-BLAST. Iteration approach is utilized in LAST-MUD and the iteration number is equal to the number of the transmit antennas in the system. At each iteration, the symbol with maximum post-detection *signal-to-noise ratio* (SNR) is detected and eliminated from the received signals. The detailed description of the LAST-MUD algorithm [35] is as follows:

for $i = 1$ to L (4.3*a*)

$$k_i = \arg \min_{j \notin \{k_1, \cdots, k_{i-1}\}} [\mathbf{R}(i)^+]_{(j,j)} \tag{4.3b}$$

$$\mathbf{w}_{k_i} = [\mathbf{R}(i)^+]_{k_i} \tag{4.3c}$$

$$z_{k_i} = \mathbf{w}_{k_i}^H \mathbf{Y}(i) \tag{4.3d}$$

$$\hat{b}_{k_i} = \psi(z_{k_i}) \tag{4.3e}$$

if $i \le L-1$ (4.3*f*)

for $p = 1$ to P (4.3*g*)

$$\mathbf{r}_p(i+1) = \mathbf{r}_p(i) - [\mathbf{X}_p(i)]_{k_i} \hat{b}_{k_i} \tag{4.3h}$$

end (4.3*i*)

obtain $\mathbf{X}_p(i+1)$ and $\mathbf{R}(i+1)$ (4.3*j*)

$$\mathbf{Y}(i+1) = \sum_{p=1}^{P} \mathbf{X}_p(i+1)^H \mathbf{r}_p(i+1) \qquad (4.3k)$$

end (4.3*l*)

end. (4.3*m*)

Here, i denotes the ith iteration, "+" denotes the Moore-Penrose pseudoinverse and $\psi(\bullet)$ means hard decision. In this case, the pseudoinverse matrix is equal to the inverse matrix. The notation $[\mathbf{R}(i)^+]_{(l,j)}$ represents the element at the lth row and the jth column of the matrix $[\mathbf{R}(i)^+]$. The operations $[\mathbf{R}(i)^+]_{k_i}$, $[\mathbf{X}_p(i)]_{k_i}$ mean taking out the k_i th column from matrix $\mathbf{R}(i)^+$, $\mathbf{X}_p(i)$ and form the new column vectors respectively. $\mathbf{X}_p(i+1)$ and $\mathbf{R}(i+1)$ are obtained, respectively, by striking out the k_ith column of $\mathbf{X}_p(i)$ and the k_i th row and column of $\mathbf{R}(i)$.

The LAST-MUD algorithm consists of four steps, namely, determination of the optimal ordering (4.3*b*), nulling vector computation (4.3*c*), signal estimation ((4.3*d*), (4.3*e*)) and interference cancellation ((4.3*f*) ~ (4.3*l*)).

Equation (4.3*b*) shows the selection criterion of the detected symbol in each iteration. In each iteration, the detected symbol is the one with the highest post-detection signal-to-noise ratio (SNR), which is the symbol corresponding to the minimum value of the diagonal line in matrix $[\mathbf{R}(i)^+]$. The proof of this statement is shown as follows.

In each iteration, substitute (4.3*k*) into (4.3*d*), the soft decision z_{k_i} can be rewritten as

$$\begin{aligned} z_{k_i} &= \mathbf{w}_{k_i}^H \mathbf{Y}(i) \\ &= \mathbf{w}_{k_i}^H (\mathbf{R}(i)\mathbf{b} + \tilde{\mathbf{n}}(i)) \end{aligned}$$

$$= \mathbf{w}_{k_i}^H (\mathbf{R}(i)\mathbf{b} + \sum_{p=1}^{P} \mathbf{X}_p^H(i)\mathbf{n}_p)$$

$$= \mathbf{w}_{k_i}^H \mathbf{R}(i)\mathbf{b} + \mathbf{w}_{k_i}^H \sum_{p=1}^{P} \mathbf{X}_p^H(i)\mathbf{n}_p$$

$$= b_{k_i} + \mathbf{w}_{k_i}^H \sum_{p=1}^{P} \mathbf{X}_p^H(i)\mathbf{n}_p \,. \tag{4.4}$$

The post-detection SNR is

$$\frac{E[\|b_{k_i}\|^2]}{E[\left\|\mathbf{w}_{k_i}^H \sum_{p=1}^{P} \mathbf{X}_p^H(i)\mathbf{n}_p - E[\mathbf{w}_{k_i}^H \sum_{p=1}^{P} \mathbf{X}_p^H(i)\mathbf{n}_p]\right\|^2]} \,. \tag{4.5}$$

Because $\mathbf{n}_p$ is a complex-valued zero-mean Gaussian random N-length vector, thus $E[\mathbf{w}_{k_i}^H \sum_{p=1}^{P} \mathbf{X}_p^H(i)\mathbf{n}_p] = 0$. Also $E[\|b_{k_i}\|^2]$ is a positive constant, so the value of post-detection SNR is inverse proportional to the value of $E[\left\|\mathbf{w}_{k_i}^H \sum_{p=1}^{P} \mathbf{X}_p^H(i)\mathbf{n}_p\right\|^2]$.

$$E[\left\|\mathbf{w}_{k_i}^H \sum_{p=1}^{P} \mathbf{X}_p^H(i)\mathbf{n}_p\right\|^2]$$

$$= E[(\mathbf{w}_{k_i}^H \sum_{p=1}^{P} \mathbf{X}_p^H(i)\mathbf{n}_p)(\mathbf{w}_{k_i}^H \sum_{p=1}^{P} \mathbf{X}_p^H(i)\mathbf{n}_p)^H]$$

$$= E[(\mathbf{w}_{k_i}^H \sum_{p=1}^{P} \mathbf{X}_p^H(i)\mathbf{n}_p)((\sum_{p=1}^{P} \mathbf{n}_p{}^H \mathbf{X}_p^H(i))\mathbf{w}_{k_i})^H]$$

$$= \mathbf{w}_{k_i}^H \sigma^2 \mathbf{R}(i)\mathbf{w}_{k_i}$$

$$= \sigma^2 [\mathbf{R}(i)^+]_{(k_i,k_i)}, \tag{4.6}$$

here σ^2 is a positive constant. Because $\mathbf{R}(i)$ is a semi-positive definite hermitian matrix, so $\mathbf{R}(i)^+$ is also a semi-positive definite hermitian matrix and its diagonal components are non-negative real values. Thus, (4.5) and (4.6) show that the maximum value of the post-detection SNR is obtained when $[\mathbf{R}(i)^+]_{(k_i,k_i)}$ has the smallest value, which proves the detected symbol selection criterion of each iteration in LAST-MUD.

4.3 B-Chase and L-Chase Detectors over MIMO-CDMA Systems

From Section 4.2, the equation (4.2) $\mathbf{Y} = \mathbf{Rb} + \tilde{\mathbf{n}}$, which is the sufficient statistic vector, is similar to the equation (2.28) $\mathbf{r} = \mathbf{Hb} + \mathbf{n}$, the received signal vector in the V-BLAST system. Both of them are written as the sum of a noise vector and the product of a matrix and transmitted signals. The processing operation principle of $\mathbf{Y}$ in LAST-MUD is exactly the same as the received signal in V-BLAST. This similarity motivates the idea of using some advanced techniques used for improving the performance of V-BLAST to enhance the performance of LAST-MUD. Among the advanced schemes used to improve the performance of V-BLAST, one important category consists of Chase based detectors [12], which include the B-Chase and L-Chase detectors. In this section, we investigate the use of these two Chase based schemes in MIMO-CDMA systems.

The idea of using the Chase algorithm in MIMO-CDMA system would be like this: the different detected symbols have different decision reliabilities that are related to the post-detection SNR. The smaller post-detection SNR one symbol has, the more unreliable its decision is. Therefore, we can try different values for the least reliable

symbol and get several candidate hard decision vectors. The number of the candidate vectors is assumed to be q. Among the candidate vectors, the final hard decision vector will be the one satisfying a cost function

$$\arg\min_{\hat{\mathbf{b}}_k \in \{\hat{\mathbf{b}}_1,\cdots,\hat{\mathbf{b}}_q\}} \sum_{p=1}^{P} \left\| \mathbf{r}_p - \mathbf{X}_p \hat{\mathbf{b}}_k \right\|^2 \tag{4.7}$$

4.3.1 B-Chase Detector

Similar to [12], the detailed process of the B-Chase detector of a MIMO-CDMA system is described below and its block diagram is shown in Fig. 4.2.

Step 1: Decide the first detected symbol.

The index of the first detected symbol is assumed to be j and $j \in \{1,\cdots,L\}$. For simplicity, we use the symbol that has the maximum value in the diagonal line of $[\mathbf{R}(1)^+]$ as the first detected symbol. This symbol is the least reliable one in the first iteration,

Step 2: Create the candidate value list $\{\hat{b}_{j,1},\cdots,\hat{b}_{j,q}\}$ for the jth symbol.

The value q is the size of signal modulation constellation. Here, QPSK modulation is assumed and q=4.

Step 3: Cancel the contribution of the jth symbol from received symbol $r_m(1)$ and determine the residual vector $\mathbf{r}'_{m,k}(2)$:

$$\mathbf{r}'_{m,k}(2) = \mathbf{r}_m(1) - b_{j,k}(\mathbf{X}_m(1))_j \tag{4.8}$$

here, $m \in \{1,\cdots,P\}$, $k \in \{1,\cdots,q\}$.

Step 4: Send $\{\mathbf{r}_{1,k}(2),\cdots,\mathbf{r}_{P,k}(2)\}$ to its corresponding sub-detector and make the decision about the left $L-1$ symbols.

The sub-detector is as same as LAST-MUD. Combine the first detected symbol $\hat{b}_{j,k}$, the output of k th sub-detector is a candidate hard decision vector $\hat{\mathbf{b}}_k$.

Step 5: Choose $\hat{\mathbf{b}}_k$ satisfying the cost function (4.7) as the final decision $\hat{\mathbf{b}}$.

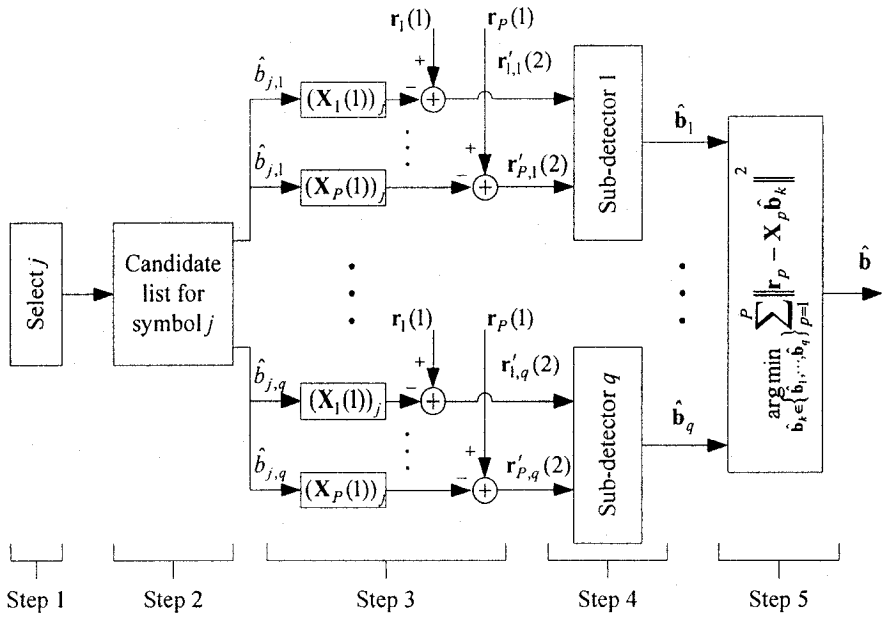

Figure 4.2 The block diagram of the B-Chase detector in MIMO-CDMA system

4.3.2 L-Chase Detector

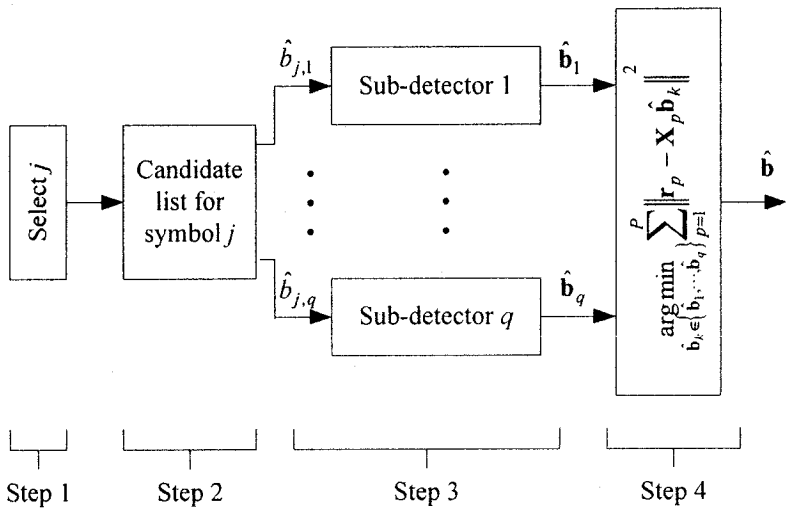

Figure 4.3 The block diagram of the L-Chase detector in MIMO-CDMA system

The block diagram of the L-Chase detector is shown in Fig. 4.3. Several steps of the L-Chase detector are exactly the same as the steps of the B-Chase detector. The L-Chase detector only has two differences from the B-Chase detector. The first one is that there is no step 3 of the B-Chase detector in the L-Chase detector, i.e. the candidate values $\{\hat{b}_{j,1}, \cdots, \hat{b}_{j,q}\}$ are sent to sub-detectors directly. The second one is the sub-detector's operation of L-Chase focuses on estimating and cancelling the noise terms, which is quite different from the operation of the B-Chase sub-detector. Similar to [12], [36], the detailed description of the operation is demonstrated below.

Let

$$\mathbf{c} = \mathbf{R}^{+}\mathbf{Y} = \mathbf{R}^{+}(\mathbf{R}\mathbf{b} + \tilde{\mathbf{n}}) = \mathbf{I}_L \mathbf{b} + \tilde{\mathbf{n}}', \tag{4.9}$$

where $\mathbf{I}_L$ denotes the $L \times L$ identity matrix and $\mathbf{c} = [c_1, \ldots, c_L]^T$, $\tilde{\mathbf{n}}' = \mathbf{R}^{+}\mathbf{n} = [\tilde{n}_1', \cdots, \tilde{n}_L']^T$ are the length L vectors.

In the L-Chase detector, inside each sub-detector, the noise term of the first detected jth symbol is

$$\tilde{n}'_{j,k} = c_j - \hat{b}_{j,k},\ k \in \{1, \cdots, q\}. \tag{4.10}$$

Assume that the index of other symbols is i and $i = 1, \cdots, j-1, j+1, \cdots, L$. The idea of the L-Chase detector is to estimate the noise term $\tilde{n}'_i$ in (4.9) by using (4.10) and subtract the estimated $\tilde{n}'_i$ from c_i. After that, better decision of the ith symbol could be made.

The decision of other symbols inside one sub-detector is

$$b_{i,k} = dec\{c_i - p_{i,k}\tilde{n}_j\} = dec\{c_i - p_{i,k}(c_j - \hat{b}_{j,k})\}, \tag{4.11}$$

where $p_{i,k}$ is the prediction coefficient. When $\hat{b}_{j,k}$ is correct, the noise variance of the ith symbol is

$$\begin{aligned}
&E[\left|\tilde{n}'_{i,k} - p_{i,k}\tilde{n}'_{j,k}\right|^2] \\
&= E[\left|\tilde{\mathbf{r}}_i\tilde{\mathbf{n}} - p_{i,k}\tilde{\mathbf{r}}_j\tilde{\mathbf{n}}\right|^2] \\
&= E[(\tilde{\mathbf{r}}_i\tilde{\mathbf{n}} - p_{i,k}\tilde{\mathbf{r}}_j\tilde{\mathbf{n}})(\tilde{\mathbf{r}}_i\tilde{\mathbf{n}} - p_{i,k}\tilde{\mathbf{r}}_j\tilde{\mathbf{n}})^H] \\
&= E[(\tilde{\mathbf{r}}_i - p_{i,k}\tilde{\mathbf{r}}_j)\tilde{\mathbf{n}}\tilde{\mathbf{n}}^H(\tilde{\mathbf{r}}_i - p_{i,k}\tilde{\mathbf{r}}_j)^H] \\
&= (\tilde{\mathbf{r}}_i - p_{i,k}\tilde{\mathbf{r}}_j)\sigma^2\mathbf{R}(\tilde{\mathbf{r}}_i - p_{i,k}\tilde{\mathbf{r}}_j)^H,
\end{aligned} \tag{4.12}$$

where the L length vector $\tilde{\mathbf{r}}_i$ is the ith row of $\mathbf{R}^+$, the superscript H denotes Hermitian. When $p_{i,k}\tilde{\mathbf{r}}_j$ is the projection of $\tilde{\mathbf{r}}_i$ onto $\tilde{\mathbf{r}}_j$, the noise variance is minimized. Therefore the ith prediction coefficient is

$$p_{i,k} = \tilde{\mathbf{r}}_i\tilde{\mathbf{r}}_j^* / \left\|\tilde{\mathbf{r}}_j\right\|^2, \tag{4.13}$$

here "*" is the conjugate sign. Substitute (4.13) into (4.11), the hard decision values for other symbols within the kth sub-detector are

$$b_{i,k} = dec\{c_i - \tilde{\mathbf{r}}_i \tilde{\mathbf{r}}_j^{*}(c_j - b_j)/\|\tilde{\mathbf{r}}_j\|^2\}. \tag{4.14}$$

4.3.3 Simulation Results

In this section, the simulation of LAST-MUD, the B-Chase detector and the L-Chase detector is carried out. QPSK modulation, i.e. $q = 4$, is used in all cases. The number of user groups is $G = 12$ and the spreading factor $N = 32$ is assumed. Spreading codes are generated randomly and perfect channel estimation is assumed. Two cases, the number of each user's transmit antennas M is less than and equal to the number of receive antennas P, are considered for all three detectors. The performance comparisons of LAST-MUD and the B-Chase detector, LAST-MUD and the L-Chase detector are shown in Fig. 4.4, and Fig. 4.5 respectively. From these simulation results, we know the B-Chase detector can outperform LAST-MUD. When the number of one user transmit antennas is equal to the number of receive antennas, the performance improvement is especially significant. But the L-Chase detector, which can achieve better performance than V-BLAST in single user situation, is inferior to LAST-MUD. Reviewing the theoretical deduction in Subsection 4.3.2, the problem of the L-Chase detector is caused by the choice of the prediction coefficient $p_{i,k}$. The prediction coefficient is only one data: in single user situation, the dimension of vectors $\tilde{\mathbf{r}}_i$, $\tilde{\mathbf{r}}_j$ is small, the estimation of noise term has high accuracy; however, in multiuser situation, the dimension of vector $\tilde{\mathbf{r}}_i$

is large, the estimation of noise term has a big error. Therefore, the performance of the L-Chase detector is even worse than LAST-MUD.

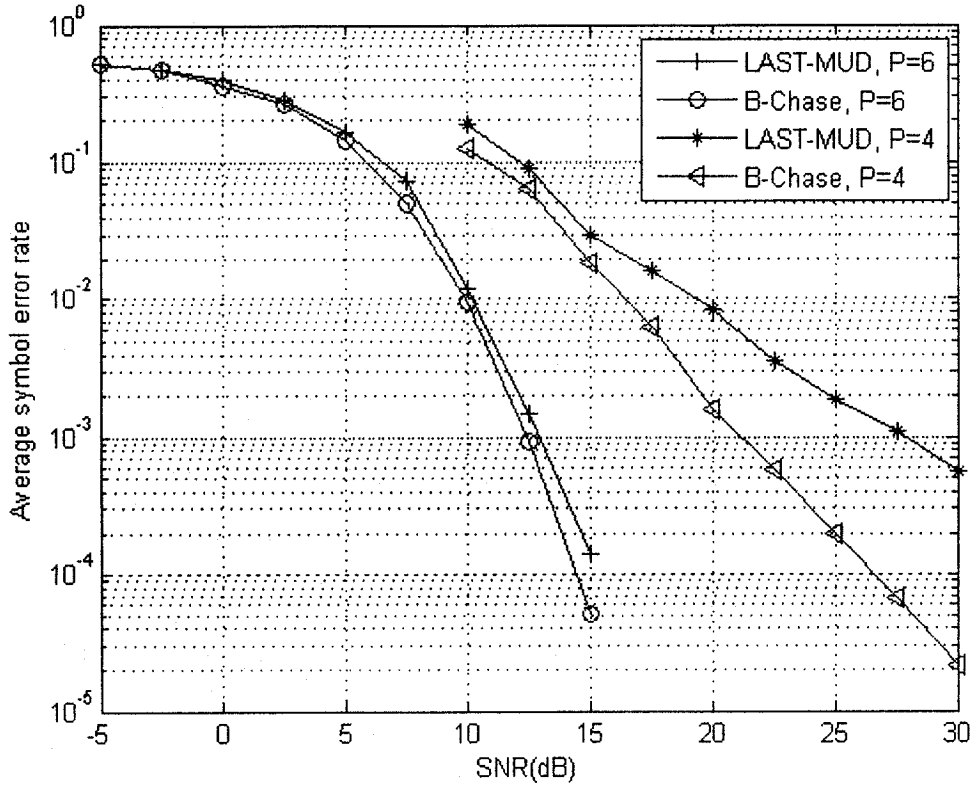

Figure 4.4 Performance comparison: the B-Chase detector and LAST-MUD (M=4, G=12, N=32)

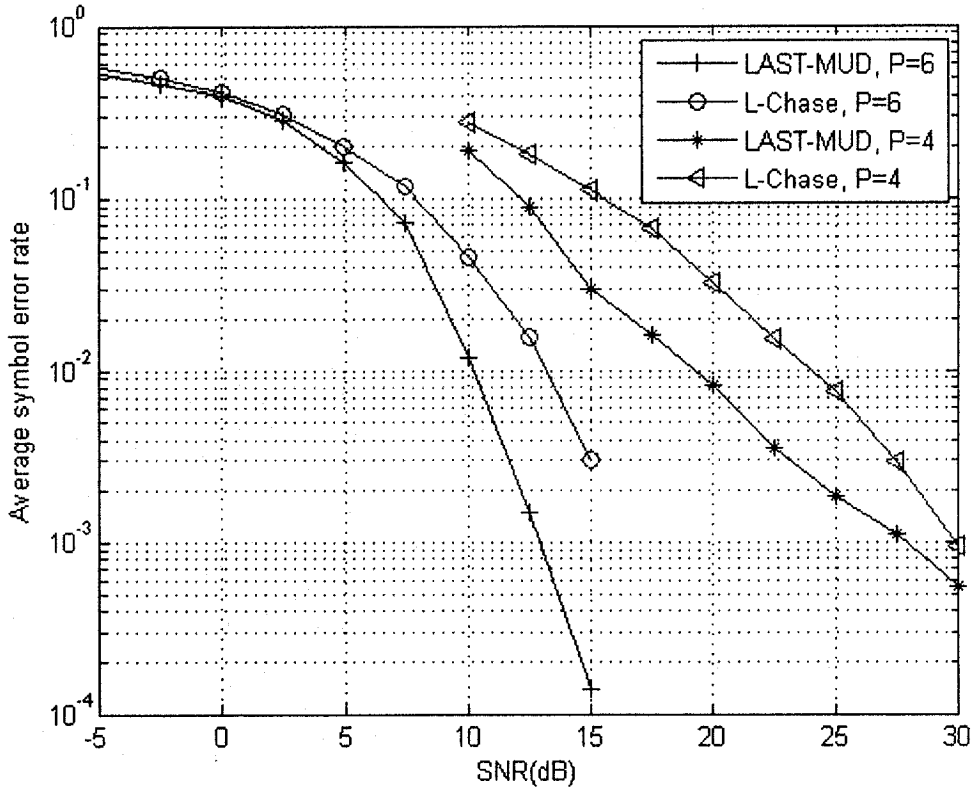

Figure 4.5 Performance comparison: the L-Chase detector and LAST-MUD (M=4, G=12, N=32)

4.4 Proposed Chase Based MIMO-CDMA Detector

In the B-Chase detector, the symbol that we consider as the weakest one is in fact only the most unreliable symbol at the first iteration, but it may not be the weakest one in the whole detection procedure of LAST-MUD. In this section, we first do the performance analysis of LAST-MUD, which shows the weakest detected symbol among the whole LAST-MUD procedure. After that, a new Chase based scheme that focuses on ameliorating the error probability of the weakest symbol is proposed.

4.4.1 Performance Analysis of Layered Space-Time Multiuser Detector

In this subsection, we extend the analysis in [37] to the performance analysis of the LAST-MUD over a MIMO-CDMA system.

The probability of the decision vector $\hat{\mathbf{b}}$ being different from the transmitted vector $\mathbf{b}$ can be expressed as:

$$P_{LAST-MUD} = \sum_{\mathbf{b}\in\Omega^L} P(\hat{\mathbf{b}} \neq \mathbf{b}, \mathbf{b}) = \sum_{\mathbf{b}\in\Omega^L} P(\hat{\mathbf{b}} \neq \mathbf{b}|\mathbf{b})P(\mathbf{b})$$

$$= \sum_{\mathbf{b}\in\Omega^L} (1 - P(\hat{\mathbf{b}} = \mathbf{b}|\mathbf{b}))P(\mathbf{b}), \tag{4.15}$$

here, Ω represents the signal modulation constellation with size q; $P(\mathbf{b})$ is the probability that the symbol vector $\mathbf{b} = [b_1, \cdots, b_L]^T$ is transmitted; $P(\hat{\mathbf{b}} \neq \mathbf{b}|\mathbf{b})$, $P(\hat{\mathbf{b}} = \mathbf{b}|\mathbf{b})$ are the conditional probability that the decision vector $\hat{\mathbf{b}}$ is incorrect and correct respectively when $\mathbf{b}$ is transmitted. Since $P(\hat{\mathbf{b}} = \mathbf{b}|\mathbf{b})$ is independent of the symbol being transmitted, therefore $P(\hat{\mathbf{b}} = \mathbf{b}|\mathbf{b})$ is constant and we have

$$P_{LAST-MUD} = 1 - P(\hat{\mathbf{b}} = \mathbf{b}|\mathbf{b}). \tag{4.16}$$

Using chain rule in $P(\hat{\mathbf{b}} = \mathbf{b}|\mathbf{b})$, we have

$$P(\hat{\mathbf{b}} = \mathbf{b}|\mathbf{b})$$

$$= P((\hat{b}_{k_1} = b_{k_1}, \cdots, \hat{b}_{k_L} = b_{k_L})|\mathbf{b})$$

$$= P(\hat{b}_{k_1} = b_{k_1}, \cdots, \hat{b}_{k_L} = b_{k_L}, \mathbf{b}) / P(\mathbf{b})$$

$$= P(\hat{b}_{k_L} = b_{k_L} \left| (\mathbf{b}, \hat{b}_{k_1} = b_{k_1}, \cdots, \hat{b}_{k_{L-1}} = b_{k_{L-1}})) P(\mathbf{b}, \hat{b}_{k_1} = b_{k_1}, \cdots, \hat{b}_{k_{L-1}} = b_{k_{L-1}}) / P(\mathbf{b}) \right.$$

$$= P(\hat{b}_{k_L} = b_{k_L} \left| (\mathbf{b}, \hat{b}_{k_1} = b_{k_1}, \cdots, \hat{b}_{k_{L-1}} = b_{k_{L-1}})) P(\hat{b}_{k_1} = b_{k_1}, \cdots, \hat{b}_{k_{L-1}} = b_{k_{L-1}} \right| \mathbf{b})$$

$$= P(\hat{b}_{k_L} = b_{k_L} \left| (\mathbf{b}, \hat{b}_{k_1} = b_{k_1}, \cdots, \hat{b}_{k_{L-1}} = b_{k_{L-1}})) \cdots P(\hat{b}_{k_2} = b_{k_2} \right| \mathbf{b}, \hat{b}_{k_1} = b_{k_1}) P(\hat{b}_{k_1} = b_{k_1} \left| \mathbf{b} \right.)$$

$$= \prod_{i=1}^{L} P(\hat{b}_{k_i} = b_{k_i} \left| (\mathbf{b}, \hat{b}_{k_1} = b_{k_1}, \cdots, \hat{b}_{k_{i-1}} = b_{k_{i-1}})) \right. . \tag{4.17}$$

Substituting (4.17) into (4.16), we have,

$$1 - P(\hat{\mathbf{b}} = \mathbf{b} \left| \mathbf{b} \right.)$$

$$= 1 - \prod_{i=1}^{L} P(\hat{b}_{k_i} = b_{k_i} \left| (\mathbf{b}, \hat{b}_{k_1} = b_{k_1}, \cdots, \hat{b}_{k_{i-1}} = b_{k_{i-1}})) \right.$$

$$= 1 - \prod_{i=1}^{L} (1 - P(\hat{b}_{k_i} \neq b_{k_i} \left| (\mathbf{b}, \hat{b}_{k_1} = b_{k_1}, \cdots, \hat{b}_{k_{i-1}} = b_{k_{i-1}}))) \right.$$

$$\approx \sum_{i=1}^{L} P(\hat{b}_{k_i} \neq b_{k_i} \left| (\mathbf{b}, \hat{b}_{k_1} = b_{k_1}, \cdots, \hat{b}_{k_{i-1}} = b_{k_{i-1}})) \right. , \tag{4.18}$$

here, the final result is an approximation that ignores the product terms since the error probabilities are small at high SNR.

The variable z_{k_i} in (4.4) has a Gaussian distribution if the interference corresponding to the detected symbols is cancelled entirely. Consequently, the error probability of $\hat{b}_{k_i} \neq b_{k_i}$ given that the previously detected symbols are correct can be expressed as:

$$P_i = P(\hat{b}_{k_i} \neq b_{k_i} \left| (\mathbf{b}, \hat{b}_{k_1} = b_{k_1}, \cdots, \hat{b}_{k_{i-1}} = b_{k_{i-1}})) = Q\left(\frac{d}{2\sigma_{LAST\text{-}MUD}}\right) \right. , \tag{4.19}$$

where, d is the minimum distance between any two signal constellation points. Letting $x = \frac{d}{2\sigma_{LAST-MUD}}$ and using the formula in [38], (4.19) can be approximated as

$$P_i = Q(x)$$

$$= \left(\frac{1}{(1-1/\pi)x + (1/\pi)\sqrt{x^2+2\pi}} \right) \frac{1}{\sqrt{2\pi}} \exp\left(\frac{-d^2}{4\sigma^2 [\mathbf{R}(i)^+]_{(k_i,k_i)}} \right). \quad (4.20)$$

Due to the fast decay of the exponential function, at high SNR, i.e., when d^2/σ^2 is large, $P_{LAST-MUD}$ are dominated by a single term

$$\left(\frac{1}{(1-1/\pi)x + (1/\pi)\sqrt{x^2+2\pi}} \right) \frac{1}{\sqrt{2\pi}} \exp\left(\frac{-d^2}{4\sigma^2 \max\limits_{k_i} [\mathbf{R}(i)^+]_{(k_i,k_i)}} \right). \quad (4.21)$$

In another word, the symbol corresponding to $\max\limits_{k_i} [\mathbf{R}(i)^+]_{(k_i,k_i)}$ is the weakest one that has the highest possibility to be wrongly detected.

4.4.2 Proposed Chase Based Detector

Our proposed Chase based detector concentrates on alleviating the adverse effect of the weakest symbol in LAST-MUD. The symbols detected before the weakest one are kept intact and q candidate values for the weakest symbol are created, where q is the size of modulation signal constellation. Consequently, q subdetectors are established for deciding the subsequent symbols after the weakest one. Combining the symbols detected in the subdetectors and the symbols detected before the weakest symbol, q candidate

vectors are produced. Finally, the vector minimizing the cost function (4.7) is chosen as the final decision vector.

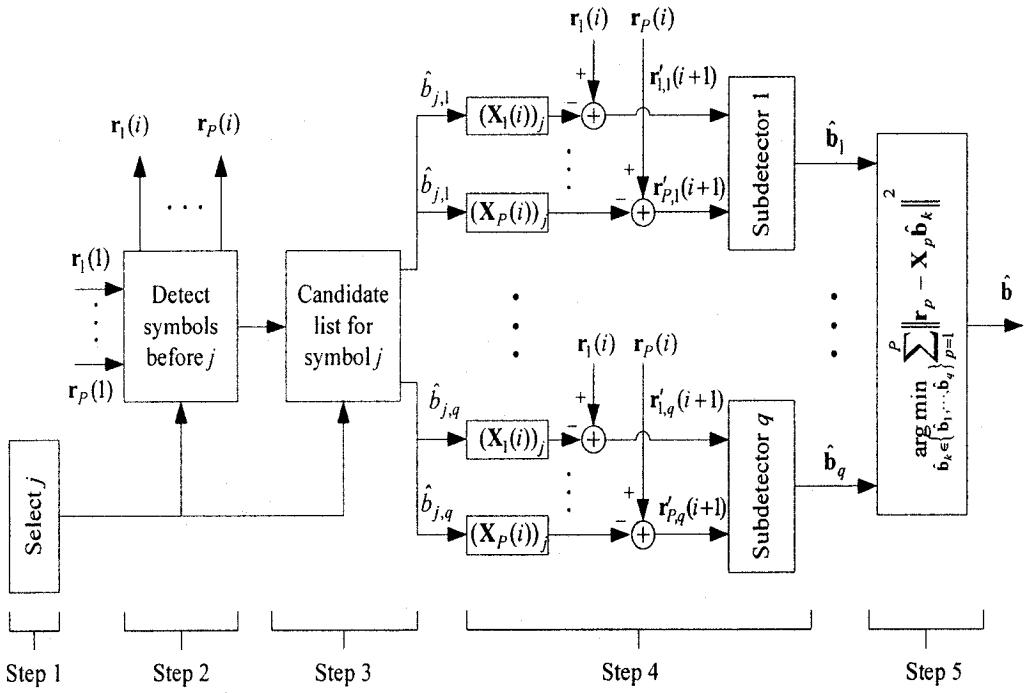

Figure 4.6 The block diagram of the proposed Chase detector.

The proposed Chase based detector is shown in Fig. 4.6. The detailed description is:

Step 1: Search for the weakest symbol in LAST-MUD.

This symbol corresponds to $\max[\mathbf{R}(i)^+]_{(k_i,k_i)}$ and its index is denoted as j, $j \in \{1,\cdots,L\}$.

Step 2: Detect the symbols preceding the weakest symbol using LAST-MUD.

Step 3: Create the candidate list $\{b_{j,1},\cdots,b_{j,q}\}$ when detecting the weakest symbol.

Step 4: Cancel the contribution of the weakest symbol from the leftover received symbol $\mathbf{r}_m(i)$ and determine the residual vector $\mathbf{r}'_{m,k}$: $\mathbf{r}'_{m,k}(i+1) = \mathbf{r}_m(i) - b_{j,k}(\mathbf{X}_m(i))_j$, $m \in \{1, \cdots, P\}$, $k \in \{1, \cdots, q\}$. Send the residual symbols to q subdetectors.

Each subdetector is as same as LAST-MUD. Combining the symbols detected before the weakest one, the output of the kth subdetector is a candidate hard decision vector $\hat{\mathbf{b}}_k$.

Step 5. Choose $\hat{\mathbf{b}}_k$ satisfying the cost function (4.7) as the final decision.

The B-Chase detector and the proposed scheme have the same cost function and subdetectors. The different parts of these two approaches are the weakest symbol selection criterion and the location to detect the weakest symbol. In the B-Chase detector, the weakest symbol is chosen as the first symbol to be detected and q candidate values are created for it. The weakest symbol selection criterion in B-Chase is that the symbol with minimum post-detection SNR in the first iteration, i.e. the symbol with the maximum value in the diagonal of $[\mathbf{R}(1)^+]$ is chosen as the weakest one.

Compared to the B-Chase detector, our proposed Chase scheme has the following two advantages:

- The choice of the most unreliable symbol is more in line with the Chase algorithm. In the B-Chase detector, the symbol that we consider as the weakest one is in fact only the most unreliable symbol at the first iteration, but it may not be the weakest one in the whole detection procedure of LAST-MUD. In our proposed scheme, the weakest symbol, which is represented by a candidate list, is exactly the weakest one during the whole procedure of LAST-MUD.

- The proposed scheme has less complexity. The B-Chase detector constructs q subdetectors at the beginning of the detection process. However, the proposed scheme constructs q subdetectors after we have detected the weakest symbol. Compared to the B-Chase detector, the interference cancellation in $q-1$ subdetectors before detection of the weakest symbol is avoided.

4.4.3 Simulation Results

In this subsection, the simulation of LAST-MUD, the B-Chase detector and our proposed Chase detector is carried out. QPSK modulation, i.e. $q = 4$, is used in all cases. The number of user groups is $G = 12$ and the spreading factor $N = 32$ is assumed. Spreading codes are generated randomly and perfect channel estimation is assumed. The performance for the condition when the number of each user's transmit antennas M is less than the number of receive antennas P is shown in Fig. 4.7. The case for $M = P$ is shown in Fig. 4.8. In both situations, the proposed scheme and the B-Chase detector outperform LAST-MUD. The performance improvement is significant when $M = P$. From Fig. 4.8, we observe the phenomena: at low SNR, the performance of the proposed scheme is a little worse than the B-Chase detector; while at high SNR, the proposed scheme attains better performance compared to the B-Chase detector. These phenomena are consistent with the performance analysis in Subsection 4.4.1. The higher is the SNR, it is more likely that the error occurs at the weakest symbol. Since the proposed scheme exactly concentrates on this weakest symbol, at high SNR, better accuracy can be attained. In the B-Chase detector, the detection error that we try to correct is not

necessarily the weakest one, therefore its performance is not as good as the proposed scheme at high SNR. From a theoretical point of view, this phenomenon should also exist when $M < P$. But it is not significant due to the limited performance improvement.

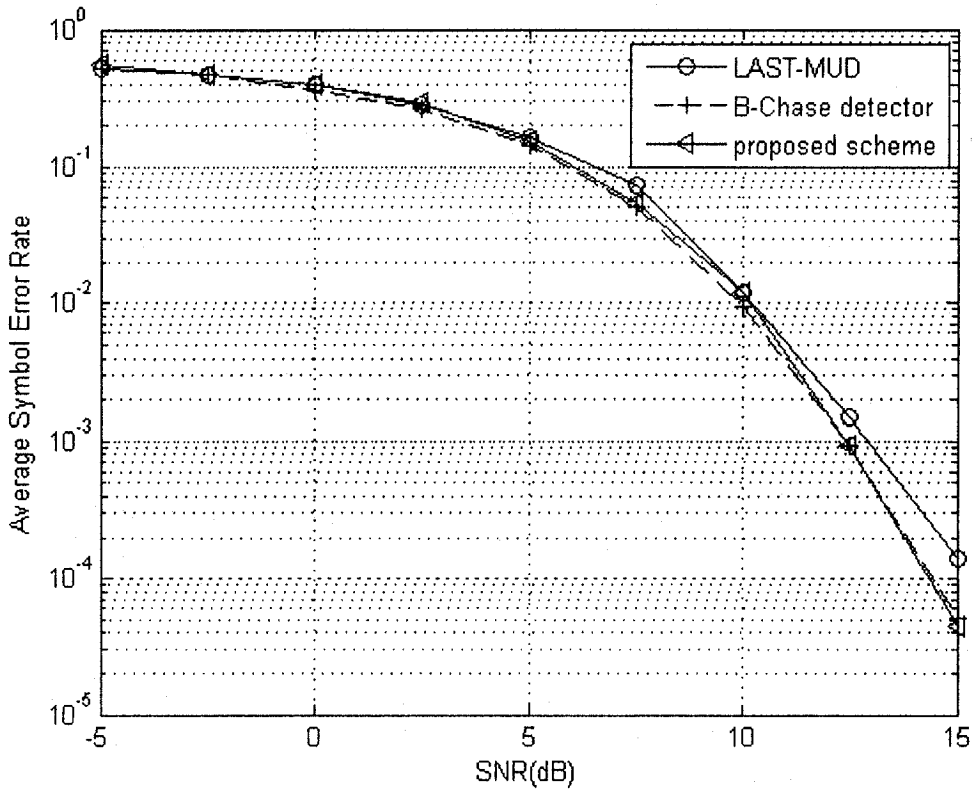

Figure 4.7 Performance comparison: LAST-MUD, B-Chase and the proposed scheme (M=4, P=6, G=12, N=32).

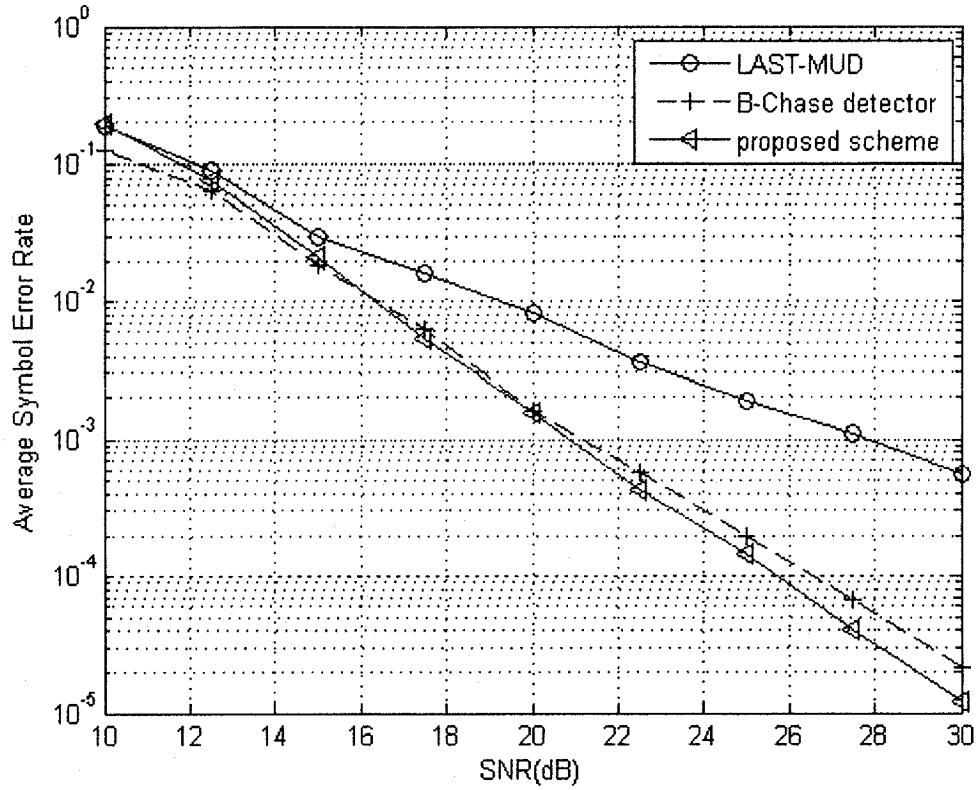

Figure 4.8 Performance comparison: LAST-MUD, B-Chase and the proposed scheme(M=4, P=4, G=12, N=32).

4.5 Summary

In this chapter, the approach that uses the Chase algorithm to improve the performance of MIMO-CDMA multiuser detector is studied. First, the B-Chase and L-Chase detectors, which are two advanced Chase based detectors and can achieve performance enhancement in single user V-BLAST systems, are applied to LAST-MUD. The simulation results show that the B-Chase detector can outperform LAST-MUD but the performance of the L-Chase detector is worse than LAST-MUD due to the wrong noise estimation. And then, a new Chase based MIMO-CDMA multiuser detector scheme,

which focuses on reducing the error decision in detecting the weakest symbol in LAST-MUD, is proposed. Simulation results and analysis show that the proposed scheme can achieve a better performance than LAST-MUD. When the number of transmit antennas of each user is equal to the number of receive antennas, the improvement is especially significant. Compared to the B-Chase detector, the proposed scheme has less complexity and has the tendency of achieving a better performance at high SNR.

CHAPTER 5

CONCLUSIONS AND FUTURE WORKS

5.1 Conclusions

In this thesis, we develop some Chase based multiuser detectors in SISO-CDMA and MIMO-CDMA uplink systems.

In SISO-CDMA systems, we propose a new multistage parallel interference cancellation (PIC) scheme that uses the *normalized least-mean-square* (NLMS) algorithm in the earlier stages and the Chase algorithm in the later stages. The simulation and complexity analysis, which are carried out over synchronous and asynchronous Rayleigh fading Channels, show that the proposed scheme can achieve a better performance than multistage NLMS-PIC but with less complexity.

In MIMO-CDMA systems, we propose a new Chase based multiuser detection scheme over synchronous Rayleigh fading channels. The proposed approach provides performance gain by concentrating on improving the detection accuracy of the weakest symbol. Compared to the *layered space-time multiuser detector* (LAST-MUD), the

proposed scheme can achieve substantial performance improvement, especially, when the number of transmit antennas is equal to the number of receive antennas. As a comparion to our proposed scheme, we also apply the B-Chase and L-Chase approaches to MIMO-CDMA systems. The B-Chase and L-Chase detectors were originally proposed for improving the performance of the *vertical Bell Laboratories layered space-time* (V-BLAST) system. The B-Chase detector can achieve better performance than LAST-MUD, but the performance of L-Chase is even worse than LAST-MUD due to the wrong noise estimation. The problem existing in the B-Chase detector is the criterion for selecting the weakest symbol. In our scheme, a more reasonable selection criterion is proposed. We show that the proposed scheme has less complexity than the B-Chase detector but with the tendency of achieving better performance at high SNR.

5.2 Future Works

In this section, some topics for future study are presented:

- Applying a layered space-time technique to each group instead of to all users can significantly reduce the complexity of LAST-MUD. Therefore, for reducing the complexity, it is worthwhile to study the proposed MIMO-CDMA detection scheme by using group detection technique.
- For the proposed MIMO-CDMA detector, we only considered the case with synchronous fading channels. To analyse and simulate the proposed MIMO-CDMA detector in asynchronous fading channels is one of the future works.

- In this thesis, we showed that the performance of the MIMO-CDMA L-Chase detector is not as good as LAST-MUD due to the wrong noise estimation. However, its low complexity makes this approach very attractive in real life implementation. So modifying the noise estimation criterion on the L-Chase detector could be a direction.
- In an actual system, the implementation of a receiver can be done by *digital signal processors* (DSP) or *field-programmable gate arrays* (FPGA). Therefore another direction is to work on the implementation of our schemes on DSP and FPGA.

Bibliography

[1] Lawrence Harte, Dave Bowler, *Introduction to Mobile Telephone Systems: 1G, 2G, 2.5G, and 3G Wireless Technologies and Services*. ALTHOS Publishing Inc, 2004.

[2] Andrews, J.G., "Interference Cancellation for Cellular Systems: A Contemporary Overview," *IEEE Wireless Communications Magazine*, vol. 12, no. 2, Apr. 2005, pp. 19-29.

[3] S. Verdú, *Multiuser Detection*, 1st edition, Cambridge, 1998.

[4] S. Moshavi, "Multi-User Detection for DS-CDMA Communications," *IEEE Communications Magazine*, vol. 34, no. 10, Oct. 1996, pp. 124-36.

[5] E. Telatar, "Capacity of Multi-antenna Gaussian Channels," *European Transactions on Telecommunications*, vol. 10, no.6, Nov./Dec. 1999, pp. 585-595.

[6] G. J. Foschini and M. J. Gans, " On Limits of Wireless Communications in a Fading Environment When Using Multiple Antennas," *Wireless Personal Communications*, vol. 6, 1998, pp. 311-335.

[7] C. E. Shannon, "A Mathematical Theory of Communication," *Bell System Technical Journal*, vol. 27, pp. 379-423 (Part one), pp. 623-656(Part two), Oct. 1948, reprinted in book form, University of Illinois Press, Urbana, 1949.

[8] V. Tarokh, A. Naguib, N. Seshadri and A.R.Calderbank, "Space-time Codes for High Data Rate Wireless Communication: Performance criteria in the Presence of Channel Estimation Errors, Mobility, and Multiple Paths," *IEEE Transactions on Communications*, vol. 47, no. 2, pp. 199-207, Feb. 1999.

[9] Branka Vucetic and Jinhong Yuan, *Space-Time Coding*. Wiley, 2003.

[10] D. Chase, "A class of algorithms for decoding block codes with channel measurement information," *IEEE Transactions on Information Theory*, pp. 170-182, Jan. 1972.

[11] G. Q. Xue, J. F. Wang, T. Le-Ngoc, and S. Tahar, "Adaptive multistage parallel interference cancellation for CDMA," *IEEE Journal on Selected Areas in Communications*, vol. 17, pp. 1815- 1827,Oct. 1999.

[12] D. W. Waters and J. R. Barry, "The Chase family of detection algorithm for multiple-input multiple-output channels," *IEEE Global Communications Conference*, vol. 4, pp. 2635-2639, Nov, 2004.

[13] G. J. Foschini, G. D. Golden, R. A. Valenzuela, and P. W. Wolaniansky, "Simplified processing for high spectral efficiency wireless communication employing multi-element arrays," *IEEE Journal on Selected Areas in Communications*, vol. 17, pp. 1841-1852, Nov. 1999.

[14] J. G. Proakis, *Digital Communications*. 4th edition, New York: Mcgraw-Hill, 2001.

[15] K. S. Schneider, "Optimum Detection of Code Division Multiplexed Signals," *IEEE Transactions on Aerospace and Electronic Systems*, vol. AES-15, no., Jan. 1979, pp. 181-85.

[16] R. Kohno, M. Hatori, and H. Imai, "Cancellation Techniques of Co-Channel Interference in Asynchronous Spread Spectrum Multiple Access Systems," *Electronics and Communications in Japan*, vol. 66-A, no. 5, May 1983, pp. 20-29.

[17] R. Lupas and S. Verdú, "Near-Far Resistance of Multi-User Detectors in Asynchronous Channels," *IEEE Transactions on Communications*, vol. 38, no. 4, Apr. 1990, pp. 496-508.

[18] R. Lupas and S. Verdú, "Linear Multi-User Detectors for Synchronous Code-Division Multiple-Access Channels," *IEEE Transactions on Information Theory*, vol. 35, no. 1, Jan. 1989, pp. 123-36.

[19] Z. Xie, R. T. Short, and C. K. Rushforth, "A Family of Suboptimum Detectors for Coherent Multi-User Communications," *IEEE Journal on Selected Areas in Communications*, vol. 8, no.4 May 1990, pp. 683-90.

[20] A. J. Viterbi, " Very Low Rate Convolutional Codes for Maximum Theoretical Performance of Spread-Spectrum Multiple-Access Channels," *IEEE Journal on Selected Areas in Communications*, vol. 8, no.4, May 1990, pp. 641-49.

[21] R. Kohno et al., "Combination of an Adaptive Array Antenna and a Canceller of Interference for Direct-Sequence Spread-Spectrum Multiple-Access System," *IEEE Journal on Selected Areas in Communications*, vol. 8, no. 4, May 1990, pp. 675-82.

[22] M. K. Varanasi and B. Aazhang, "Multistage Detection in Asynchronous Code-Division Multiple-Access Communications," *IEEE Transactions on Communications*, vol. 38, no. 4, Apr. 1990, pp. 509-19.

[23] D. Divsalar, M. K. Simon, and D. Raphaeli, "Improved parallel interference cancellation for CDMA," *IEEE Transactions on Communications*, vol. 46, pp. 258-268, Feb. 1998.

[24] S. M. Alamouti, "A Simple Transmit Diversity Technique for Wireless Communications," *IEEE Journal on Selected Areas in Communications*, vol. 16, no. 8, pp. 1451-1458, Oct. 1998.

[25] V. Tarokh, H. Jafarkhani and A. R. Calderbank, "Space-Time Block Codes from Orthogonal Designs," *IEEE Transactions on Information Theory*, vol. 45, no. 5, pp. 1456-1467, July 1999.

[26] V. Tarokh, H. Jafarkhani and A. R. Calderbank, "Space-Time Block Coding for Wireless Communications: Performance Results," *IEEE Journal on Selected Areas in Communications*, vol. 17, no. 3, pp. 451-460, Mar. 1999.

[27] V. Tarokh, N. Seshadri and A. R. Calderbank, "Space-Time Codes for High Data Rate Wireless Communication: Performance Criterion and Code Construction," *IEEE Transactions on Information Theory*, vol. 44, no. 2, pp. 744-765, Mar. 1998.

[28] G. J. Foschini, "Layered Space-Time Architecture for Wireless Communication in A Fading Environment When Using Multiple Antennas," *Bell Labs Technical Journal*, vol. 1, p. 41-59, Autumn 1996.

[29] P. W. Wolnainsky, G. J. Foschini, G. D. Golden, and R. A. Valenzuela, "V-BLAST: An Architecture for Achieving Very High Data Rates Over The Rich-Scattering Wireless Channel," *International Symposium on Signals, Systems and Electronics*, Pisa, pp. 295-300, Italy, 1998.

[30] K. Sheikh, D. Gesbert, D. Gore, and A. Paulraj, "Smart Antennas for Broadband Wireless Access Networks," *IEEE Communications Magazine*, vol. 37, pp. 100-106, Nov. 1999.

[31] M. O. Damen, H. E. Gamal, and G. Caire, "On Maximum-Likelihood Detection and the search for the Closest Lattice Point," *IEEE Transactions on Information Theory*, vol. 49, no. 10, Oct. 2003.

[32] D. Wübben, R. Böhnke, V. Kühn, and K. Kammeyer, "Near-Maximum-Likelihood Detection of MIMO Systems Using MMSE-Based Lattice-Reduction," *IEEE International Conference on Communications*, vol. 2, pp. 798-802, June. 2004.

[33] S. Verdú, "Minimum probability of error for asynchronous Gaussian multipleaccesschannels," *IEEE Transactions on Information Theory*, vol. 32, pp. 85-96, Jan. 1986.

[34] S. Sfar, R. D. Murch, and K. B. Letaief, "Achieving high capacities in CDMA systems using multiuser detection based on BLAST," *IEEE International Conference on Communications*, vol. 2, pp. 565-569, June, 2001.

[35] S. Sfar, R. D. Murch, and K. B. Letaief, "Layered space-time multiuser detection over wireless uplink systems," *IEEE Transactions on Wireless Communications*, vol. 2, no. 4, pp. 653-668, Jul. 2003.

[36] D. W. Waters and J. R. Barry, "Partial decision-feedback detection for multiple-input multiple-output channels," *IEEE International Conference on Communications*, vol. 5, pp. 2668-2672, June, 2004.

[37] Y. Li, and Z. Luo, "Parallel detection for V-BLAST system," *IEEE International Conference on Communications*, vol. 1, pp.340-344, May 2002.

[38] Alberlo Leon-Garcia, *Probability and Random Processes for Electrical Engineering*, 2nd edition, Addison-Wesley, 1994.